UNIVERSITAT POLITÈCNICA DE CATALUNYA
BARCELONATECH

SUPERVISORY CONTROL DESIGN FOR MICROGRID ENERGY MANAGEMENT OPTIMIZATION BASED ON RENEWABLE GENERATION AND CONSUMPTION FORECASTING

A Master's Thesis
Submitted to the Faculty of the
Escola Tècnica d'Enginyeria de Telecomunicació de Barcelona
Universitat Politècnica de Catalunya
By

Camilia Oukit

In partial fulfilment
Of the requirements for the degree of
MASTER IN ELECTRONICS ENGINEERING

Advisor: Francesc Guinjoan
Co-Advisor: Martin Marietta

Barcelona, July 2017

Title of the thesis: Supervisory control design for microgrid energy management optimization based on renewable generation and consumption forecasting

Author: Camilia Oukit

Advisors: Francesc Guinjoan, Martin Marietta

Abstract:

Solar-based electricity production has become an essential part of the general energy production in the recent years with the will to use more renewable sources. The one issue that appears is the uncertainty of the solar irradiation. It is then more complicated to predict the energy generated in the future times.

The Energy Management System used on the grid schedules the energy exchanges between the devices based on the prediction of the state of the system in the next time interval. The Model Predictive Control forecasts the power produced as well as that of the energy demand from the load and defines the state of the system. In order to minimize the corresponding cost function, this forecast should be as accurate as possible, with the minimum prediction error.

To address these forecasting needs, we will extract some data from a database using an algorithm directly connected to the server. And we will compute the remaining values using an accurate forecasting method, the Simple Average. Then, for this information to be even more precise, we use the Rolling Horizon approach, that enables a regular updating of the forecast. Simulation results and experiments confirm the influence of some parameters on the prediction error and hence on the cost function.

Keywords:

Photovoltaic generation, Irradiation, Forecasting methods, Optimization of a cost function, Model predictive control, Rolling Horizon.

To my parents, my family and my friends that were here for me all this time

Acknowledgments:

I first would like to express my gratitude to my supervisors, Francesc Guinjoan, electronic engineering expert professor, and Martin Marietta, PHD student at Universitat Politecnica de Catalunya (UPC). Thank you for giving me the opportunity to work on this project and providing me with all the information and guidance that I needed. Both allowed this paper to be my own work, and I am thankful for that.

A very special gratitude goes to Meritxell Lamarca, from Signal theory and Communications department, that offered her help and explained to me different concepts of data processing.

I would also like to acknowledge my university in France, INSA de Lyon, that offered me the possibility to go on an exchange year and carry out this master thesis at the electronics department of the UPC. I met interesting people and had remarkable conversations with the professors and PHD students here in Barcelona.

Finally, I would express my very profound gratitude to my parents, my family and friends for providing me with unfailing support and continuous encouragement throughout the process of research and writing of my thesis. This accomplishment would not have been possible without them. Thank you once again.

Camilia Oukit

Table of Contents

List of figures

List of tables

I. Introduction: Application framework & objectives

I.1 System under study

An energy transition is taking place since the past few years in response to the challenges regarding climate change and the overuse of sources of energy. A transformation of the energy management strategies became mandatory. As fossil resources represent the highest share in the world energy production until now, the actual energy system is vulnerable. The supply is limited and the demand increasing tremendously. The impact on global warming is also an issue and many countries and organizations are working towards more sustainable solutions.

The development of solar-based electricity production, particularly in the photovoltaics form, has increased significantly in the recent years. Many reasons can explain this evolution. Yet, many challenges represent obstacles for a total and efficient solar energy integration. One main challenge is the uncertainty of the solar irradiation, which makes it harder to predict how much energy can be produced on a smaller scale such as a day, an hour or a minute. Research is guided towards developing tools and algorithms that can manage this instability of solar power by bringing better forecasting methods for example.

This work is based on a real case microgrid taken from the MEDsolar project (Machrek Energy Development-Solar) initiative [Annex 1]. The project was developed in some countries of Machrek area: Jordan, Lebanon and Palestine with the objective to face some problems regarding the quality of their electrical supply. In particular, the weakness in their electrical generation and distribution systems like the impossibility to increase the contracted power and the frequent blackouts of the main grid that leads to the intensive use of the diesel generation with the consequent provisioning-dependence of diesel fuel from foreign countries. The objective of the MEDsolar project is to reduce the operation cost of the system and at the same time the use of expensive and pollutant energy sources, by introducing commercial devices for PV generation and electrical energy storage.

The figure below shows the configuration of the microgrid under study for the Lebanon microgrid proposed in [1] [2].

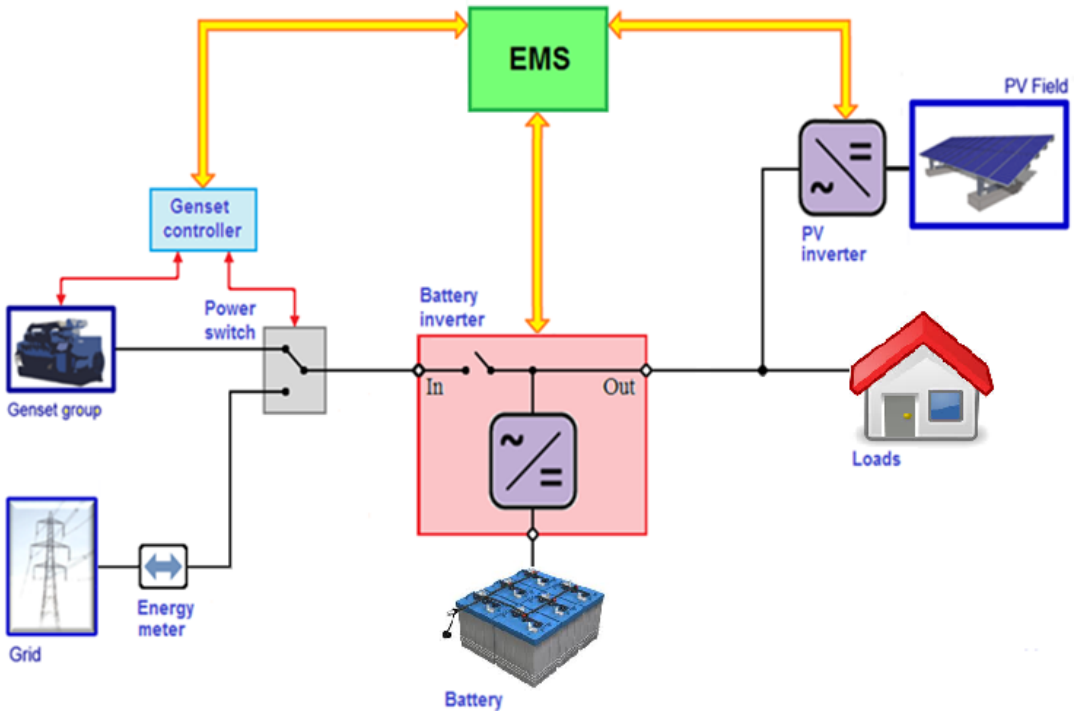

Figure 1: Microgrid configuration

The microgrid under study considers initial facilities: the main grid and a diesel generator group that operates as a backup and can be activated by an automatic switch. With the introduction of the PV generation-batteries, the loads could be supplied by the mains, the diesel generator or from the battery as voltage sources or by the PV generator as current source [3][4]. Additionally, a bidirectional converter is needed to manage the charge and discharge process of batteries and an overall supervisory control namely EMS (Energy Management System) which can set the power references to the controllable devices which are the Diesel generator, the bidirectional converter, the maximum PV power and the power switch.

I.2 Description of the EMS

The philosophy of the EMS management is Model Predictive Control (MPC) in which the design is based on control actions obtained from the optimization of a criteria[5][7]. This criteria is related with the future system behaviour that is predicted by a model. It is the objective function included in the optimization model. In this case, it represents the economic result: cost-incomes of the MG operation during a time period, that must be minimized [6]. The EMS operation is at the highest level of the hierarchical control structure detailed in [10].

The typical architecture considers several constraints as physical operating limits of the energy system, energy balances and the tariff structure of the service-grid. The forecasted values of demand and PV generation are obtained from the irradiation data

provided by external interfaces. Some measurements on site like the battery SOC and the energy taken from the grid are needed as it is shown in Figure 2.

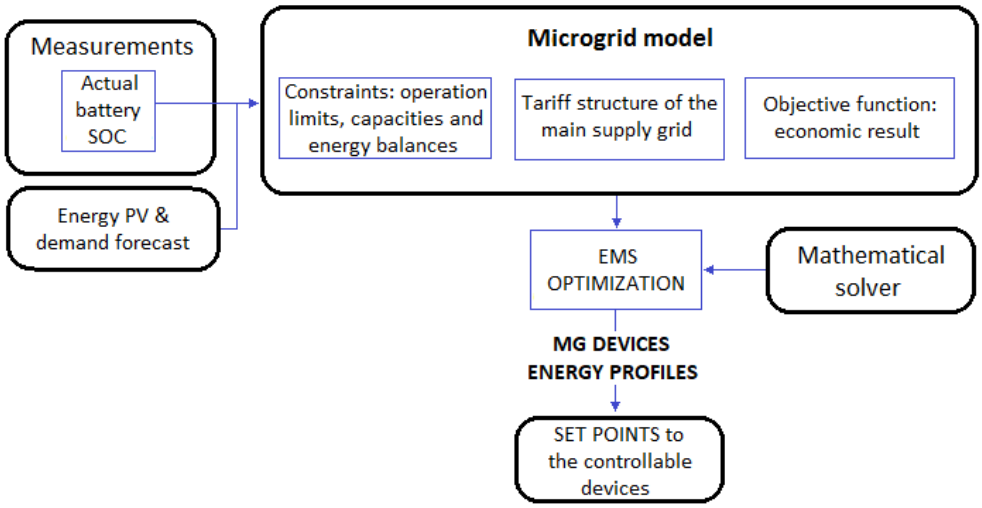

Figure 2: Typical EMS architecture

In a general framework, the time treatment consists on a long prevision time period (horizon) that is subdivided in smaller time-discrete slots in which all the inputs: the constraints, the forecast data and the objective function are computed. As a result of solving the optimization model, an optimal schedule for all the devices (controllable and not) are obtained but only the information of the first time-interval (t1) is used to determine the immediate power references for the controllable units while the data for the subsequent time intervals are discarded. A Rolling Horizon strategy within the MPC approach is then applied and after a time period equal to the time slot duration, a new set of microgrid measurements and forecast updates are taken into account for a new optimization process when new power references are obtained.

The EMS online operation is as follows: the supervisory control receives the forecasting data of power and loads from one side, and the data of the system itself (the real grid energy contribution and the state of charge of the battery from the other side). From this information, and using the cost function we mentioned before, the EMS performs the optimization and proposes a scenario so that the cost is minimized while the loads are fully supplied. This scenario is given in the form of instructions for all the devices. The idea is to schedule in advance where the energy should be taken from and which devices it should supply (or stored if needed). Then, in the next iteration, the whole process starts again.

More specifically, before the EMS implementation, when the network is connected to the public electricity distribution system, it configures by itself the source of voltage and the corresponding frequency for the best performance functioning. The idea is that the network can only have two states: Connected to the grid, or isolated from it.

In the case of connection with the grid, the system is stable, and usually it does not meet any problem. However, in the case of a black-out, the network is automatically disconnected from the grid, and connected to the diesel generator instead. The stability problem occurs here as not enough diesel is provided hence not all loads are supplied.

With the use of this energy management system, the general functioning is different. As one of the requirements is to avoid the use of diesel generators, both for environmental and availability reasons, and to focus on renewable sources of energy (photovoltaic in the scope of this project), the EMS is configured in this way:

The EMS is also responsible for the different elements it is controlling. That is to say, it verifies constantly that all the restrictions concerning each of the devices, the loads and the grid are met. This enables a better management of the maintenance, as the lifetime of the equipment is extended by avoiding useless deterioration. But also because units availability can be determined ahead of time when the equipment needs to be replaced or repaired. Furthermore, the EMS can generate the needed energy profiles for each equipment so that the cost function is minimal.

The microgrid control possesses different hierarchical levels of instructions and the orders from the EMS are placed in the highest level. In a typical EMS optimization based problem, the control is done on an hourly or minutal scale, and its main goal is to set the power of the elements over time.

Due to the EMS functioning, the need to know the future evolution of the irradiance, and consequently the power from one side, and the demand in power from the other side becomes natural. Relevant forecasting data is then necessary for the optimization procedure.

As we described the EMS, it is a real-time operating system, which means that it receives data in real-time, processes it, outputs the solution and sends it to the corresponding equipment. Consequently, the EMS is constantly communicating with the rest of the network, collecting data on a regular basis.

Within the frame of the MEDsolar project, two time scales are used: the daily horizon with an hourly granularity (HSDH), and the monthly horizon with daily granularity (DSMH). This will be explained in the thesis proposal. For these two scales, the EMS will consider a certain number of parameters. We mention the PV energy prevision to be injected into the microgrid, the energy produced by the diesel generator, the energy exchanged with the mains, the energy exchanged with the battery banks, the prevision of the battery State Of Charge (SOC), and the energy to supply the loads.

These parameters will be distributed as inputs and outputs of the EMS. Concerning the inputs, the EMS will receive the following data: The forecast of the renewable energy generators output for the given time horizon, the energy demand of the loads for each granularity, the State Of Charge (SOC) of the ESS, the operational

limits of the non-renewable energy generators, the limitations of the Grid energy supply, the state of the loads, the operational limits of the PV generators and ESS.

Then, once this data is processed, the EMS has the following outputs: Control signals to connect or disconnect the loads, the charging and discharging energy profiles of the battery and the set points for the control system for each manageable source.

Finally, the EMS itself possesses some requirements that need to be met for a proper functioning. We then consider the market prices, that influence on the choice of using one energy source or another, the cost function included in a deterministic model of the microgrid energy management, which, depending on the cost of each element, will have a different optimized solution. And the battery management algorithm, that enables to decide when to charge or use the energy of the battery depending on the actual situation.

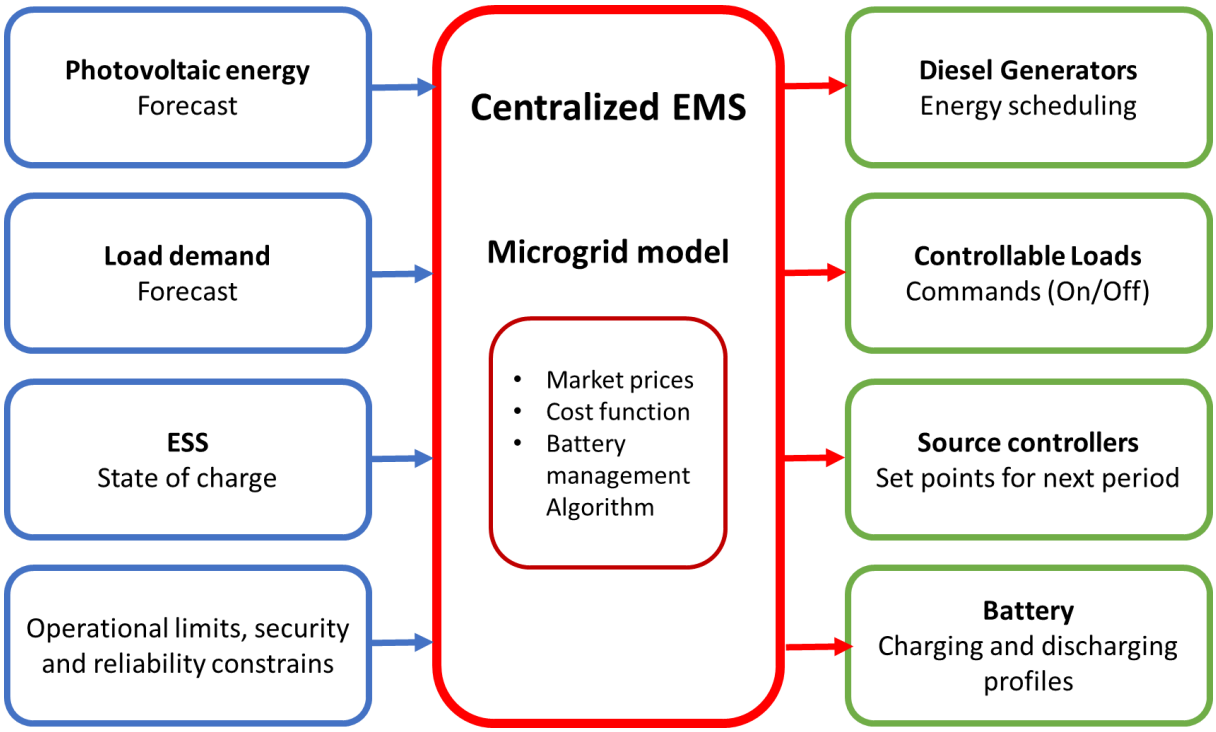

Figure 3: Inputs and Outputs of the EMS in the scope of our project

Thesis proposal

The typical MPC approach only considers one time scale. In [11], only a horizon of one day with 15 minutes intervals is discussed. In [12], a horizon of one day (24 hours) with a granularity of 10 minutes is preferred. The two times scale is contemplated in [14] but only in a daily-hourly scale and an hourly-minutal one. This work presents a novel time structure based in two scales: monthly-daily and daily-hourly. This choice was made because of the necessity to consider the pricing system existing in Lebanon that is the Incremental Block Tariff, for which, the more power you consume, the higher the unit price of the power is. We will develop the characteristics of this system later.

However, this two time-scales approach presents an issue: considering a month horizon (30 days) with a time resolution of one hour implies considering 720 variables. As this situation is high-time computation demanding because of the high volume of variables involved, the novelty of this proposal is to reduce the quantity of variables to be processed in the optimization problem resolution for the same time granularity. This situation leads to consider two different models, one for each horizon-time interval: One for the Monthly-Daily and another for the Daily-Hourly.

The quantity of variables to be considered becomes now 54 variables, which is significantly lower and hence the processing time is faster. In the next sections, the different models are detailed.

II. EMS design with the MPC approach

II.1 Algebraic representation of the models

As mentioned before, the program takes the data concerning the state of the system and the forecast values of photovoltaic generation and loads from the demand, then addresses the Model Predictive Control to analyze policies with a monthly horizon. It computes the optimal configuration such that the cost function is minimal. We will use two time scales (daily and hourly) to implement the Model Predictive Control and the Rolling Horizon. Hence, one model is needed for each scale.

For the DSMH, this is done through an algorithm that considers different parameters and the following equations:

II.1.1 Daily Scale Monthly Horizon

II.1.1.1 Photovoltaic generators (PVG)

The variable considered is the energy supply from the PV inverter (En_PVi(t)), and the related equation can be understood as if the equipment is available, the energy injected into the microgrid cannot exceed the PV generation forecast affected by the efficiency of the inverters. In other words:

$$EN\_PVi < EN\_PVifor(t) \times PVi\_eff \times HAv\_PVg(t)$$

II.1.1.2 Battery Bank (BB)

The variables considered for the Battery bank are: BB energy level (En_level(t)), BB discharging energy (En_dchg(t)), BB charging energy (En_chg(t)). The equations defining the general behavior of the battery bank are as follows:

The BB energy level must remain within the present operational limits in each time interval:

$$En\_level(t) < \frac{SOC\_up \times BB\_cap \times BB\_SOH}{100}$$

$$En\_level(t) > \frac{SOC\_low \times BB\_cap \times BB\_SOH}{100}$$

Moreover, the variation of the level of charge of the battery depends on the energy charged and discharged in the first time-interval:

$$\frac{En\_dchg(t)}{BB\_eff} - En\_chg(t) = \frac{SOC\_t0 \times BB\_cap \times BB\_SOH}{100} - En\_level(t)$$

And the variation of the level of charge of the battery depends on the energy charged and discharged in rest of the time interval

$$\frac{En\_dchg(t)}{BB\_eff} - En\_chg(t) = En\_level(t\text{-}1) - En\_level(t)$$

Also, the energy level at the end of the horizon must be the present value

$$En\_level(t) = \frac{SOC\_tf \times BB\_cap \times BB\_SOH}{100}$$

Finally, the battery charging energy must be equal to the input energy affected by the BC efficiency:

$$En\_chg(t) = En\_MGtBC(t) \times BCC\_eff$$

II.1.1.3 Bidirectional converter (BC)

Two parameters are considered for the bidirectional converter: The energy supply to the BC (En_MGtBC(t)), and the Energy supply from the BC (En_BCtMG(t)).

The equation defining the general working principle is as follows:
The output energy of the BC must be equal to the battery discharge energy affected by its efficiency:

$$En\_BCtMG(t) = En\_dchg(t) \times BCI\_eff$$

II.1.1.4 Diesel generator (DG)

The Diesel generator also considers two parameters: The energy supply from the DG (En_DG(t)), and the Diesel generator operation cost (CstOp_DG(t)).

The equations are defined as follows:

The energy delivered by the DG cannot exceed its daily maximum value set by prime power:

$$En\_GtMG < En\_DGmax \times DAv\_DG(t)$$

Two more restrictions are set assuming that in the ETD horizon there is the same behavior as the annual one:

The energy delivered by the DG in the horizon cannot exceed a percentage of the total of the prime energy:

$$\sum_{t} En\_DG(t) < En\_DGmaxH$$

The energy delivered by the DG in the horizon cannot be less than a percentage of the prime energy (recommendation not to obstruct motor):

$$\sum_{t} \text{En\_DG(t)} > \text{En\_DGminH}$$

II.1.1.5 Grid (G)

The grid considers the energy from the grid to the MicroGrid (En_GtMG(t)), the energy from the Microgrid to the grid (En_MGtG(t)), the Grid to MicroGrid energy cost on the current month (Cst_GtMG1), the Grid to MicroGrid energy cost on the next month (Cst_GtMG2), the grid energy refunds from electricity sale (Rfd_MGtG(t)) and the Grid energy consumption on the current month (En_cons1).

The equations are defined as follows:

If the MicroGrid (MG) is connected, the energy consumed from the grid cannot exceed the upper limit:

$$\text{En\_GtMG(t)} < \text{En\_GtMGmax} \times \text{DAv\_GtMG(t)}$$

And if the MG is connected, the energy injected to the grid energy cannot exceed the upper limit:

$$\text{En\_GtMG(t)} < \text{En\_GtMGmax} \times \text{DAv\_MGtG(t)}$$

II.1.1.6 Energy Balance constrains

We consider the following:

The Battery Bank is supplied from any source of energy:

$$\text{En\_DG(t)} + \text{En\_GtMG(t)} + \text{En\_PVi(t)} - (\text{En\_MGtBC(t)} + \text{EnMGtG(t)}) > 0$$

The power injection to the grid is exclusively of PV origin:

$$\text{En\_PVi(t)} - \text{En\_MGtG(t)} > 0$$

Finally, the demand must be equal to the energy supply:

$$\text{En\_Lfor(t)} = \text{En\_PVi(t)} + \text{En\_BCtMG(t)} - \text{En\_MGtBC(t)} + \text{En\_DG(t)} + \text{En\_GtMG(t)} - \text{En\_MGtG(t)}$$

II.1.1.7 Costs

Concerning the diesel operation, the cost of fuel consumption is linearly related to the electric energy produced:

$$\text{CstOp\_DG(t)} > \text{CstLin\_DG} \times \text{En\_DG(t)}$$

II.1.1.8 Economic result of purchase and sale of energy from the grid

For the current month, the prevision of the energy supply by the grid until the end of the current month must be inside of any step of the tariff system:

$$\text{En\_const0} + \sum_{t} \text{En\_GtMG(t)} < 1000000000 \times (1\text{-AV1(v)}) + \text{IUEV(v)}$$

$$\text{En\_const0} + \sum_{t} \text{En\_GtMG(t)} > \text{AV1(v+1)} + \text{IUEV(v)}$$

The sum of all the binary decision variables is 1:

$$\sum_{v} AV1(v) = 1$$

The prevision of the energy consumption in the current month is the actual consumption plus the time intervals consumption prevision:

$$\text{En\_cons1} = \text{En\_const0} + \sum_{t} \text{En\_GtMG(t)}$$

The total prevision of the energy consumption in the current month is defined as:

$$\text{Cst\_GtMG1} = \sum_{v} ((\text{En\_cons1} - \text{IUEV(v-1)}) \times \text{BT(v)} + \text{ICB(v)}) \times \text{AV1(v)}$$

For the next month, the prevision of the energy supply by the grid during the next month should be inside any step of the tariff system:

$$\sum_{t} \text{En\_GtMG(t)} < 1000000000 \times (1\text{-AV2(v)}) + \text{IUEV(v)}$$

$$\sum_{t} \text{En\_GtMG(t)} > \text{AV2(v+1)} + \text{IUEV(v)}$$

Moreover, the sum of all binary decision variables is 1:

$$\sum_{v} AV2(v) = 1$$

The total prevision of the energy consumption in the current month is defined as:

$$\text{Cst\_GtMG2} = \sum_{v} ((((En\_GtMG(t)) - IUEV(v-1)) \times BT(v) + ICB(v)) \times AV2(v))$$

The refunds for the energy injected into the main grid:

$$Rfd\_MGtG(t) = GR\_DSPr(t) \times En\_MGtG(t)$$

II.1.1.9 Objective function

The equation defining the economic result at each interval is:

$$EcnRslt(t) > CstOp\_DG(t) - Rfd\_MGtG(t)$$

Finally the total economic result is:

$$EcnRsltH = \sum_{t} EcnRslt(t) + Cst\_GtMG1 + Cst\_GtMG2$$

For the HSDH, another set of variables and equations define the general working principle.

II.1.2 Hourly Scale Daily Horizon

II.1.2.1 Photovoltaic generators (PVG)

The variable considered is the energy supply from the PV inverter (En_PVi(t)), and the related equation can be understood the same way as for the DSMH: if the equipment is available, the energy injected into the microgrid cannot exceed the PV generation forecast affected by the efficiency of the inverters. In other words:

$$En\_PVi < EN\_PVifor(t) \times PVi\_eff \times HAv\_PVg(t) \times BI\_PVg(t)$$

II.1.2.2 Battery Bank (BB)

The variables considered for the Battery bank are: BB energy level (En_level(t)), BB discharging energy (En_dchg(t)), BB charging energy (En_chg(t)). The equations defining the general behavior of the battery bank are as follows:

The BB energy level must remain within the present operational limits in each time interval:

$$En\_level(t) < \frac{SOC\_up \times BB\_cap \times BB\_SOH}{100}$$

$$En\_level(t) > \frac{SOC\_low \times BB\_cap \times BB\_SOH}{100}$$

Furthermore, the variation of the level of charge of the battery depends on the energy charged and discharged in the first time interval:

$$\frac{En\_dchg(t)}{BB\_eff} - En\_chg(t) = \frac{SOC\_t0 \times BB\_cap \times BB\_SOH}{100} - En\_level(t)$$

And the variation of the level of charge of the battery depends on the energy charged and discharged in rest of the time interval

$$\frac{En\_dchg(t)}{BB\_eff} - En\_chg(t) = En\_level(t\text{-}1) - En\_level(t)$$

Also, the energy level at the end of the horizon must be at least the present value

$$En\_level(t) > \frac{SOC\_tf \times BB\_cap \times BB\_SOH}{100}$$

Moreover, the value of the discharge energy is limited by its maximum value that is modeled as a linear function of the SOC at the start of the discharge interval

$$En\_dchg(t) < -0.62447 \times \frac{100 \times En\_level(t)}{BB\_cap \times BB\_SOH} + 270992825$$

And the range for the value of the discharge energy depends on the Bidirectional Converter

$$En\_dchg(t) > \frac{En\_BCDmin \times BCI2(t)}{BCI\_eff}$$

$$En\_dchg(t) < \frac{En\_BCDmax \times BCI2(t)}{BCI\_eff}$$

The bulk charging energy range must be within a maximum and minimum recommended values

$$En\_chg(t) < En\_BBCmax \times BCI1(t)$$
$$En\_chg(t) > En\_BBCmin \times BCI1(t)$$

Finally, the binary charge indicators of the BB cannot be 1 and 0 at the same time, as in the hourly scale the battery cannot be charging and discharging on the same time slot:

$$BCI1(t) + BCI2(t) < 1$$

II.1.2.3 Bidirectional converter (BC)

Two parameters are considered for the bidirectional converter: The energy supply to the BC (En_MGtBC(t)), and the Energy supply from the BC (En_BCtMG(t)).

The equation defining the general working principle is as follows:
The output energy of the BC must be equal to the battery discharge energy affected by its efficiency:

$$En\_BCtMG(t) = En\_dchg(t) \times BCI\_eff$$

II.1.2.4 Diesel generator (DG)

The Diesel generator also considers two parameters: The energy supply from the DG (En_DG(t)), and the Diesel generator operation cost (CstOp_DG(t)).

The equations are defined as follows:

The energy delivered by the DG cannot exceed its upper value multiplied by the availability binary variable:

$$En\_DG(t) < En\_DGmax \times BI\_DG(t)$$

The diesel generation, the hourly generation must be at least a predefined percentage of the rated capacity:

$$En\_DG(t) > \frac{ChgFct\_min}{100} \times En\_DGmax \times BI\_DG(t)$$

And the time availability determines the value of the binary state variable

$$BI\_DG(t) < HAv\_DG(t)$$

II.1.2.5 Grid (G)

The grid considers the energy from the grid to the MicroGrid (En_GtMG(t)), the energy from the Microgrid to the grid (En_MGtG(t)), the Grid to MicroGrid energy cost (Cst_GtMG), the Grid energy refunds from electricity sale (Rfd_MGtG(t)).

The equations are defined as follows:

If the MicroGrid (MG) is connected, the energy consumed from the grid cannot exceed the top value:

$$En\_GtMG(t) < En\_GtMGmax \times BI\_GR(t)$$

And if the MG is connected, the energy injected to the grid energy cannot exceed the upper limit:

$$En\_GtMG(t) > 0.0001 \times En\_GtMGmax \times BI\_GR(t)$$

The availability to receive energy from the grid determines the value of the binary state variable:

$$BI\_GR(t) < HAv\_GtMG(t)$$

The energy delivered to and received from the grid over the horizon cannot be higher than the maximum set at DSMH scale:

$$\sum_t En\_GtMG(t) < EnH\_GtMGmax$$

$$\sum_t En\_MGtG(t) < EnH\_MGtGmax$$

II.1.2.6 Loads

From the loads point of view, 3 variables are considered: The energy supply to the critical loads (En_CL(t)), the energy supply to the Non-critical Loads (En_NCL(t)) and the non-critical loads penalization cost (CstPen_NCL(t)).

And the equations describing the working principle are as follows:

First, if there is enough energy, the critical loads must be supplied:

$$EN\_CL(t) = En\_CLfor(t) \times HAv\_CL(t)$$

If enough energy is available, non-critical loads can be partially supplied:

$$EN\_NCL(t) = En\_NCLfor(t) \times HAv\_NCL(t)$$

II.1.2.7 Energy Balance constrains

We consider the following:

The Battery Bank is supplied from any source of energy:

$$En\_DG(t) + En\_GtMG(t) + En\_PVi(t) - \left(\frac{En\_chg(t)}{BCC\_eff} + EnMGtG(t)\right) > 0$$

The energy injection to the grid is exclusively of PV origin:

$$En\_PVi(t) - En\_MGtG(t) > 0$$

Finally, the energy demand must be equal to the energy supply:

$$En\_CL(t) + En\_NCL(t) = En\_PVi(t) - En\_MGtG(t) + (En\_dchg(t) \times BCI\_eff) - \frac{En\_chg(t)}{BCC\_eff} + En\_DG(t) - En\_GtMG(t)$$

Finally, the PVG delivers energy with the other energy sources (GD, grid or ESS):

$$BI\_PVg(t) < BI\_DG(t) + BI\_GR(t) + BCI1(t) + BCI2(t)$$

II.1.2.8 Costs

Concerning the diesel operation, the cost of fuel consumption is linearly related to the electric energy produced:

$$CstOp\_DG(t) > CstLin\_DG \times En\_DG(t) + CstCte\_DG \times BI\_DG(t)$$

We also consider a cost penality for not supplying the non-critical loads:

$$CstPen\_NCL(t) > PenLin\_NCL \times (En\_NCLfor(t) - En\_NCL(t))$$

II.1.2.9 Economic result of purchase and sale of energy from the grid

The cost of the supply depends on the fixed unitary price set by the DSMH

$$Cst\_GtMG(t) = CstFkWh\_GR \times En\_GtMG(t)$$

We consider as well the refunds for the sale of energy:

$$Rfd\_MGtG(t) = PrkWh\_MGtG(t) \times En\_MGtG(t)$$

II.1.2.10 Objective function

The equation defining the economic result at each interval is:

$$EcnRslt(t) > CstOp\_DG(t) + Cst\_GtMG(t) - Rfd\_MGtG(t) + CstPen\_NCL(t)$$

Finally the total economic result is:

$$EcnRsltH = \sum_{t} EcnRslt(t)$$

II.2 Photovoltaic generator power evaluation

II.2.1 Definition and working principle

The photovoltaic effect is the phenomenon that enables the conversion of light energy in electrical energy. It is based on the absorption of the photons of light rays by the semiconductor crystal, generating a number of free electrons in the crystal.

The total solar irradiance is defined as the amount of radiant energy emitted by the sun over all wavelengths, falling each second on a 1 square meter perpendicular plane outside earth at a given distance from the sun. In reality, the actual solar energy that passes through the atmosphere on earth differs from this value and depends on the position on earth (Latitude, Longitude), the moment of the year (summer, winter…), and of course the weather. This amount is called the insolation (incident solar radiation). There exist different ways to capture the solar energy, we can name the thermal systems for example, and the photovoltaic systems.

We will focus on the photovoltaic systems as these are the ones involved in our project. Photovoltaic systems capture the sun's higher frequency radiation and convert it into electrical energy. The figure below is an example of the energy captured by an array [15]:

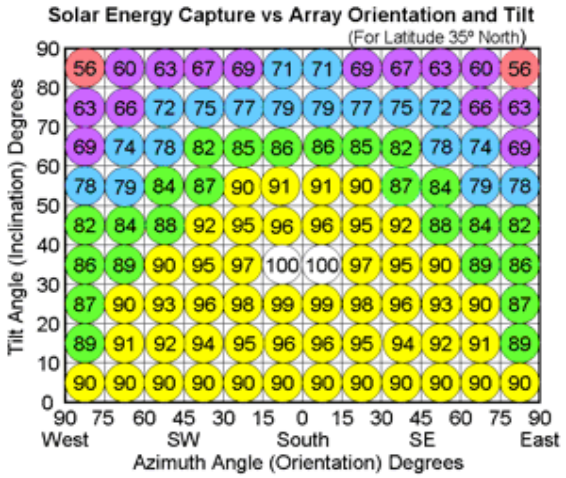

Figure 4: Evolution of an example of Solar energy capture with array positioning

In this example, the array is located at a latitude of 35º North, the optimum array orientation is pointing South and the optimum tilt is 35º, similar to the latitude. If the array system were to be mounted on a roof with a pitch of 45º on a building pointing South West, it will only receive a maximum of about 90% of the available solar energy.

The idea being to maximize the amount of energy captured, a solar tracking system can be implemented. It enables the array to "follow" the sun in its movement to catch most of the sun rays. The array is then always perpendicular to the direction of the sun. These tracking systems are automatically measuring both the azimuth and the elevation of the sun.

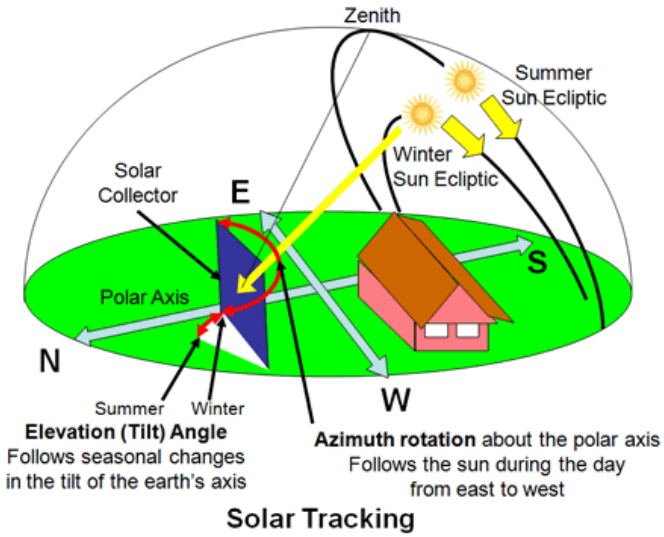

Figure 5: Representation of the Solar tracking [7]

In this figure, the general working principle of the Solar tracking is represented. We can observe both the Azimuth rotation and the Tilt Angle shown as well. This is the type of photovoltaic arrays used in the frame of the MEDsolar project. Next, we will discuss the particularities of these solar panels in terms of technical aspects.

II.2.2 Our particular case: Lebanon case

In the case of the MEDsolar project, an infrastructure is already existing and Photovoltaic panels are set. The Model used is a SunTech 300-24/Ve. Consequently, a certain number of constants and electrical characteristics are defined from the datasheet of the solar panels [Annex 2]:

Electrical Characteristics

STC	STP305-24/Ve	STP300-24/Ve	STP295-24/Ve	STP290-24/Ve
Maximum Power at STC (Pmax)	305 W	300 W	295 W	290 W
Optimum Operating Voltage (Vmp)	36.2 V	35.9 V	35.6 V	35.4 V
Optimum Operating Current (Imp)	8.43 A	8.36 A	8.29 A	8.20 A
Open Circuit Voltage (Voc)	44.7 V	44.5 V	44.3 V	44.1 V
Short Circuit Current (Isc)	8.89 A	8.83 A	8.74 A	8.65 A
Module Efficiency	15.7%	15.5%	15.2%	14,9%
Operating Module Temperature	-40 ℃ to +85 ℃			
Maximum System Voltage	1000 V DC (IEC)			
Maximum Series Fuse Rating	20 A			
Power Tolerance	0/+5 %			

STC: Irradiance 1000 W/m², module temperature 25 °C, AM=1.5;
Best in Class AAA solar simulator (IEC 60904-9) used, power measurement uncertainty is within +/- 3%

Figure 6: Extraction from the datasheet of the solar panels used in Lebanon for the MEDsolar project

We can point out some relevant data that is useful for the computation of the power generated from the irradiation received by the panels.
First, the maximum power at STC (Standard Temperature Conditions), $P_{STC} = 300\text{Wp}$ (Watt peak).
Another extraction from the datasheet gives us the following information:

Temperature Characteristics

Nominal Operating Cell Temperature (**NOCT**)	45±2°C
Temperature Coefficient of Pmax	-0.43 %/°C
Temperature Coefficient of Voc	-0.33 %/°C
Temperature Coefficient of Isc	0.067 %/°C

Figure 7: Extraction from the datasheet of the Temperature Characteristics

We can highlight some data such as the NOCT (Nominal Operating Cell Temperature):

$$NOCT = 45 \pm 2ºC$$

But also the Temperature Coefficient of Pmax, which is denominated by $k = 0.43\%/ºC$.

We also need some more data such as $n_{oth} \cong 100\%$ as it represents the losses and we will consider that there are no losses and n_{MPPT} which represents the correction of the angle of the panel following the sun direction. As in our case the panels are fixed, $n_{MPPT} \cong 100\%$.
Finally, in this location in Lebanon the number of panels used is $N_s \times N_p = 357$.
In the next section, we will present the formulation to define the power generated from the solar radiation by the photovoltaic panels.

Objectives:

This work will consist in obtaining the forecast values of the photovoltaic generation and the demand from the loads. The forecast will be done using two different sources: A direct extraction from a database using a programmed algorithm for the daily scale photovoltaic generation data [Annex 3], and a computation of the forecast values for the monthly scale photovoltaic generation and the energy demand [Annex 4]. The method used for the computation of the forecast values will be chosen among accurate methods depending on the nature of our time series.

Then, we will consider other additional techniques to improve the accuracy of the forecast for a better optimization of the cost function generated by the Energy Management System. This technique, called Rolling Horizon, will enable a smaller prediction error and hence a better organisation of the schedule for the different equipment of the network. [8][9][10]

This work will have the following structure: Chapter 3 will define the different databases, and explain how to have access to them. Then, an analysis of the times series and computations of errors will enable the choice of the most accurate forecasting method. Chapter 4 will define the Rolling Horizon approach and show how it improves the Model Predictive Control with the optimization of the cost function goal. Chapter 5 summarizes the parametric analysis done on the system. Chapter 6 presents the exploitation of this tool on some specific cases to evaluate the effect of some parameters on the cost function. Finally, section 7 details the conclusions of this work and suggests further research paths for the future.

III. Forecasting of data

III.1 Databases and Extraction

III.1.1 Definition and Extraction methods

To use the energy participation of the photovoltaic array, it is needed to consider the solar radiation and the ambient air temperature. These two elements enable the definition of the total power production by an array. The following formula expresses the power production: [19]

$$P_{mod} = P_{STC} \times \frac{G_c}{G_{STC}} \times (1 + k \cdot (T_c - T_{stc}))$$

Where

$$T_c = T_a + \frac{NOCT - 20}{800} \times G_c$$

Finally,

$$P_{PV} = N_P \times N_S \times P_{mod} \times \eta_{MPPT} \times \eta_{oth}$$

Where

P_{STC} : Rated output generated by the module under Standard Test Conditions (W)

P_{mod}: Output power of the photovoltaic module (W)

G_{STC}: Solar irradiance (W/m^2)

G_c: Irradiance of operating point (W/m^2)

k: Power temperature coefficient

T_a: Ambient temperature (ºC)

NOCT: Normal Operating Cell Temperature (ºC)

We already defined and given the constants corresponding to our case for the Photovoltaic panels in Lebanon.

We hence need the information about the total irradiance and temperature in the region we want to consider. There exist a certain number of databases that provide this kind of data. However, these databases will provide data with different scales, and under different conditions. The table below summarizes the irradiance and temperature data from a Forecast and Historical point of view. We will discuss the use of historical data in the next section.

Forecast			**Historical values**	
Irradiance	**Temperature**	**Cloud cover**	**Irradiance**	**Temperature**
Soda (Helioclim) 3 locations 1min to daily Horizon: 1 day Freq: 1/day	**Soda (NCEP)** 3 locations Every 3 hours Horizon: 3 days Freq: 3 hours	**Soda (NCEP)** 3 locations Every 3 hours Horizon: 3 days Freq: 3 hours	**NREL** 3 locations 1min to daily No limit of records Access with C code	**Intellicast** 3 locations Hourly (Tripoli) or 30min(BCN &Aalborg)
MeteoGalicia Only BCN Hourly (To Check) Horizon: 4 days Freq: 2/day	**MeteoGalicia** Only BCN Hourly (To Check) Horizon: 4 days Freq: 2/day	**MeteoGalicia** Only BCN Hourly (To Check) Horizon: 4 days Freq: 2/day		

Table 1: Databases of Irradiance, temperature and Cloud cover

Finally, depending on the source of the data, the extraction method differs. For SODA [20] Helioclim (Irradiance) for example, a Matlab code can extract a CSV file directly from the database. Of course, the extraction is not free, but we implemented a Matlab code for the free trial on the city of Carpentras in France [21][Annex 3]. The same procedure could be used for our case in Lebanon once a license is purchased.

The soda Helioclim database provides irradiance forecasting data with a horizon of 1 day, and with different granularities from 1 min to 1 day. Another database, MeteoGalicia [22], provides data with a 4-days horizon, but does not cover the Lebanon area as it is focused on the region around Spain only.

From a temperature point of view, the SODA website gives access to a database NCEP that provides with a temperature forecast every 3 hours for a horizon of 3 days in all locations. As seen from the formula of the power generated by the Photovoltaic array, the temperature effect is very small (Since k = 0.0044). Consequently, having

temperature data every 3 hours is acceptable, as having a more accurate database won't change much the value of the forecasted power.

Hence, we decide to use the SODA Helioclim for irradiance forecasting, and SODA NCEP for temperature forecasting. These forecasts will of course concern the 1-day horizon as this is the limit of the database. Regarding the other time horizon (1-month horizon and 1-day granularity), a computed forecast is proposed.

III.1.2 SODA service

SODA (**SO**lar radiation **DA**ta) is a common laboratory of MINES ParisTech and ARMINES. It offers access to a wide set of information concerning solar radiation and its use for various countries around the world.

It is an Intelligent System (IS) that generates links with other sources of information located in these countries and outputs the answer to a certain request. It uses algorithms based on data processing, data assimilation in numerical models and data fusion. The web services are provided by six different providers.

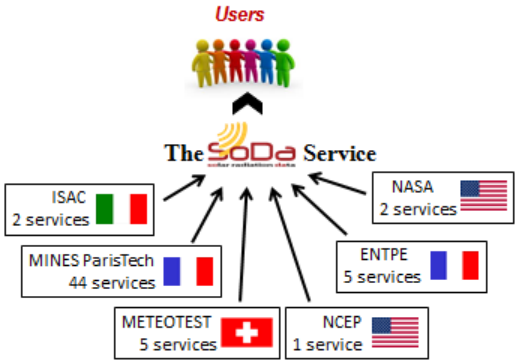

Figure 8: Providers of the SODA web service

Within the framework of our project, we will use HelioClim database (HC3 version 4 Similarity Forecast), to extract forecast irradiance data. Combining it with NCEP database (National Centers for Environmental Prediction), as it provides temperature forecasts on a long-term period (3 days).

III.2 Forecasting methods

III.2.1 Definition

Forecasting irradiance can be considered as the tool that reduces the uncertainty of the future [24] [25]. Different forecasting methods exist and can depend on different parameters. We can consider for example the forecast horizon (Long, Intermediate or Short-term forecasting), the type of data we consider…

In our case, we will work with Time series data, which assumes that data points over time have an internal structure, which should be accounted for in the analysis. We will discuss the nature of the data in the next section.

SODA proposes a forecast based on two different methods:

III.2.1.1 Similarity Model

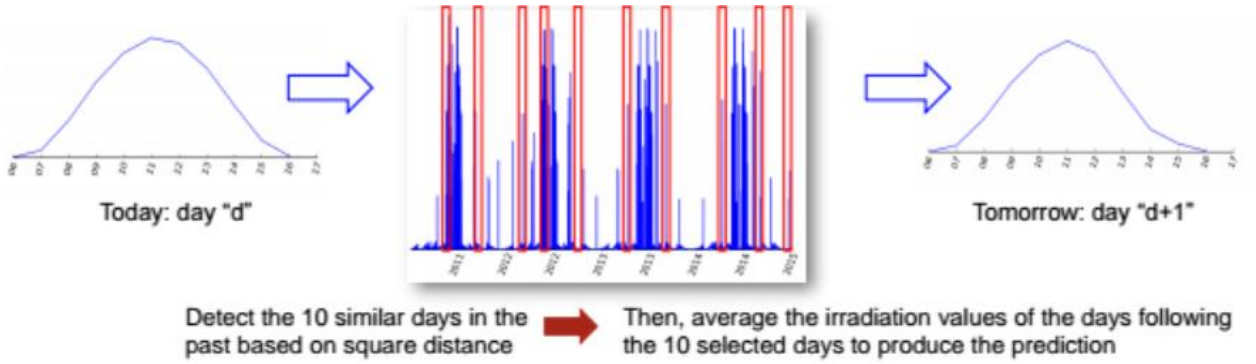

Figure 9: Illustration of the principle of the HC3v4 Similarity Forecast

The Similarity Model is based on the comparison of today's GHI (Global Horizontal Irradiance) to the past 4 years irradiance database. This model performs better in slowly varying weather areas. [Annex 4]

III.2.1.2 Persistence Model

The Persistence Model is based on satellite images, it is defined in the illustration below. It presents an example of 15min weather slots until 11:25 am. The last information we have is a half-cloudy half-sunny weather. The main assumption will be that the weather will be of the same type. Then, the next image acquired shows a nicer weather than what was planned 15min ago. The prevision is hence adjusted. This process keeps adjusting the forecast every 15min until the end of the day. [23]

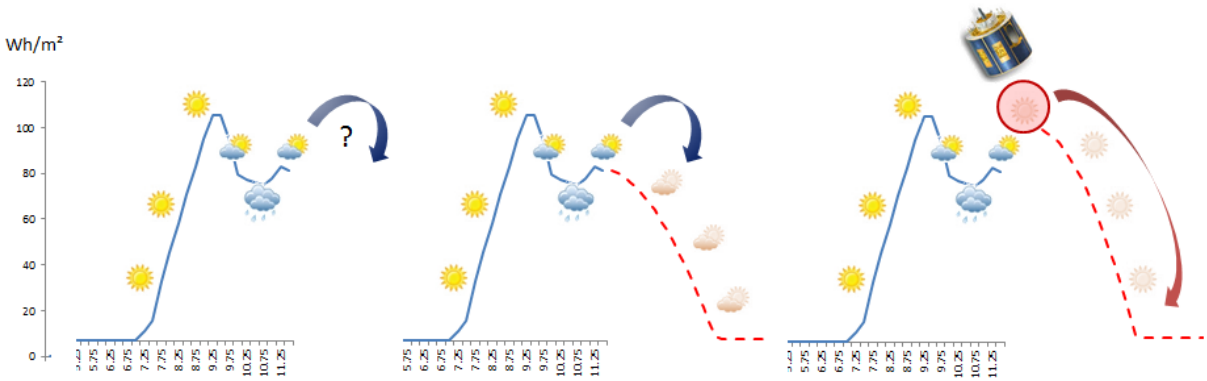

Figure 10: Illustration of the principle of the HC3v4 real-time and short-term Persistence forecast service

Experiment:

In order to verify the accuracy of these methods, we followed an experiment.

The idea is to analyse the data from a two-days extraction of irradiance and temperature. We will use SODA database Helioclim to extract the information. Choosing the "Similarity forecast" option, the system will use the Persistence model for the actual day (d), and the Similarity model for the next day (d+1).

Consequently, the process will be as follows:

The first extraction will be at $t_0 = 04{:}00$ a.m of day d and will give us the forecast values of the irradiance for d and d+1 using the Persistence model for day d, and the Similarity model for day d+1.

The next extraction will be at the end of day d at $t_1 = 09{:}00$ p.m. We will then extract the measured irradiance values for day d, as it is the past ones and hence completely known. And the forecast of day d+1 using the Persistence model again.

Finally, the last extraction will be at the end of day d+1 d at $t_2 = 09{:}00$ p.m. We will then extract the real measured irradiance values for day d+1.

These extractions will be done for hourly scale and 5-minutal scale that is averaged into hourly data. And we will compare forecast and real data using SODA database.

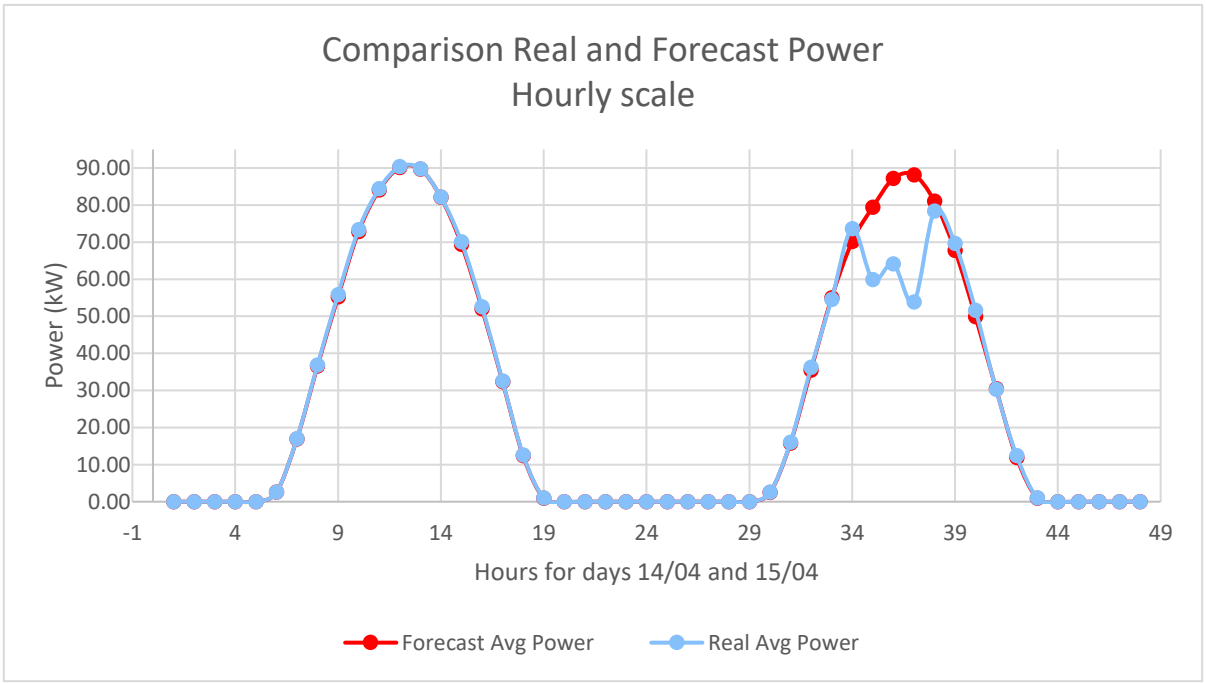

Figure 11: Evolution of Real and Forecast power on an hourly scale for 2 days

This case here is interesting, as during the 14/04/2017 and 15/04/2017 the weather conditions were unstable. Which explains the important difference between forecast and reality for the second day(d+1). However, we can notice how accurate the forecast is for day d.

Moreover, we are interested in the comparison of the hourly scale and the 5-minutal one. We hence compute the average hourly scale based on a 5-minutal one and we plot both results on the same graph:

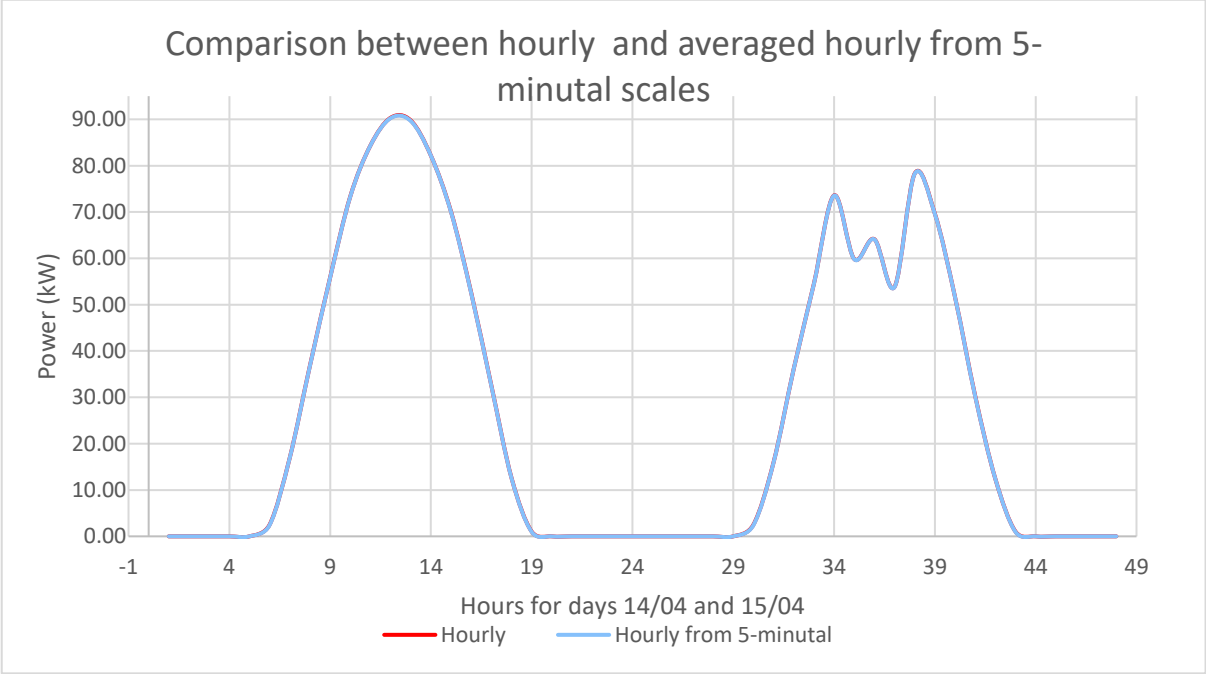

Figure 12: Evolution of power on an hourly scale and averaged hourly for 2 days

We observe that both curves superimpose, even in case of unstable weather. Furthermore, the values themselves are not totally equal as we can notice on the table below. Which means that both scales are measured separately, but are both just as accurate.

Hours 14/04	5	6	7	8	9	10	11	12	13	14	15	16	17	18	19	20
Hourly	0	2.53	16.99	36.83	55.86	73.35	84.36	90.33	89.77	82.17	70.04	52.57	32.53	12.59	1.03	0
Hourly from 5-minutal	0	2.45	16.98	36.78	55.81	73.31	84.35	90.25	89.65	82.16	69.95	52.46	32.45	12.54	0.96	0

Table 2: Power on an hourly scale and averaged hourly for 14/04. We notice that the values are not equal

When considering forecasting on a 1-day horizon, the models above, used by the SODA website on the Helioclim database, is more than enough. However, to use a 1-month horizon with 1-day granularity, a direct computation of the forecast irradiance is needed. Many techniques are used in practice. Two distinct groups of smoothing methods can be considered: Averaging methods and Exponential Smoothing methods.

III.2.2 Simple Average forecasting technique

The Simple Average technique actually computes the average of all historical data until t and uses this value as the forecast data for t+1. Which means [26]:

$$F_{t+1} = \frac{1}{t}\sum_{i=1}^{t} y_i$$

Where F_{t+1} is the forecast data and y_i is the i-th historical data.

This method is only useful when the time series presents no trends as Averaging methods are more suitable for time series data where the series is in equilibrium around a constant value (i.e. the mean). Also, Averaging methods are very useful when the time series data can be subject to random errors, as it will smooth out these errors.

III.2.3 Exponential Smoothing forecasting technique

III.2.3.1 Definition of the Exponential Smoothing

The Exponential Smoothing [26] [27] is based on the unequal weights given to the past data to define the forecast. The weights decay exponentially giving more importance to the most recent data and less to the furthest ones in time. There exist 3 different Exponential Smoothing methods: The Single Smoothing method, Holt's method and the Holt-Winters' method.

The Single Smoothing is a method where only one parameter needs to be estimated. Hence, the forecast is considered as the old value plus an adjustment for the error from the past forecast. However, Single Smoothing is not appropriate when the considered data has a trend.

To improve this situation, Holt's method was introduced, adding a new equation and a second constant. Hence Holt's method, also called Double Exponential Smoothing, enabled the forecast of data presenting a trend using 2 equations:

- The first one adjusts the actual smoothed value directly for the trend of the previous period, by adding it to the previous smoothed value, hence eliminating the lag.
- The second equation, updates the trend, i.e the difference between the two last values.

Finally, in the case our data shows trend AND seasonality, Double Exponential Smoothing does not provide an accurate forecasting anymore. A third method is proposed: Holt-Winters' method, also known as Triple Exponential Smoothing.

This method introduces another equation, and hence it is defined as:

- Overall Smoothing:

$$S_t = \alpha \frac{y_t}{I_{t-L}} + (1-\alpha)(S_{t-1} + b_{t-1})$$

- Trend Smoothing

$$b_t = \gamma(S_t - S_{t-1}) + (1-\gamma)b_{t-1}$$

- Seasonal Smoothing

$$I_t = \beta \frac{y_t}{S_t} + (1-\beta)I_{t-L}$$

- Forecast

$$F_{t+m} = (S_t + m \cdot b_t)I_{t-L+m}$$

Where:
Y is the observation
S is the smoothed observation
b is the trend factor
I is the seasonal index
F is the forecast at m periods ahead
t is an index denoting a time period
α, β and γ are constants that need to be estimated such that the error between the real and forecast data is minimized.

Once the equations for the forecast are established, we also need to initialize the method. To do so, we need at least one complete season's data to determine the initial estimates of the seasonal indices I_{t-L}.

III.2.3.2 Initialization of the method

We hence initialize the method with the following:

- Initial values of the trend factor: The slope is set to be the average of the slopes for each period:

$$b = \frac{1}{L}\left(\frac{y_{L+1} - y_1}{L} + \frac{y_{L+2} - y_2}{L} + \cdots + \frac{y_{L+L} - y_L}{L}\right)$$

- Initial values for the Seasonal Index:
  We consider we have historical data for N years of L irradiance data.
  This initialization is done following this algorithm:
  - First, we compute the average of each of the N years

$$A_N = \frac{\sum_{i=1}^{L} y_i}{L}$$

  - Then, we divide the observations by their respective mean, i.e values from y_1 to y_{365}, will be divided by A_1. From y_{366} to y_{730}, will be divided by A_2… And from $y_{1+(N-1)\times L}$ to $y_{N\times L}$, will be divided by A_N.
  - Finally, the Seasonal Indices I_N are computed as the average of each year. In other words:

$$I_N = \left(\frac{y_1}{A_1} + \frac{y_{1+1\times L}}{A_2} + \cdots + \frac{y_{1+(N-1)\times L}}{A_N}\right) \times \frac{1}{N}$$

$$I_N = \frac{1}{N} \times \sum_{i=1}^{N} \frac{y_{1+(N-1)\times L}}{A_N}$$

  Once all forecasting methods are defined and understood, we should analyse our Time Series data to decide which methods could be used.

III.3 Analysis of a time series

III.3.1 Definition

A time series [28] is a succession of observations of a same variable associated to a phenomenon, regularly spaced in time. This discrete nature of the data results from the phenomenon itself: either the information is only available at precise moments, or we submit a continuous phenomenon to a discretization or a sampling. Choosing the sampling interval has an important influence in the data and on the final results.

A time series can hence be discrete or continuous depending on the observations made. If we can predict exactly the values, we say that the series is deterministic.

If the future can only be determined partially using the past observations and cannot be forecasted precisely, we consider that the future values have a probability distribution that depend strongly on past values: The series is then considered stochastic.

A time series analysis is based on a number of properties that describe each set of observations. The first step is to plot the data and consider the following:

- If the data presents an increasing shape (Trend)

- If there exist an influence of certain periods of any time unit (Stationarity)

- If the data possesses Outliers (Discordant observations)

III.3.2 Parameters of a time series

Descriptive time series analysis is based on the idea that the variation of a series can be decomposed in a certain number of basic components. This assumption does not always lead to the most accurate results, but it is interesting if the series presents a certain trend or periodicity. Naturally, this decomposition is not unique. The parameters that we take into account when analysing a time series are the following:

III.3.2.1 Trend

It corresponds to the regular evolution during a long period of time. It can be recognized with the smooth movement of the series on a large scale, either increasing or decreasing. We usually represent this evolution with either a linear or exponential form.

Trend expresses the general movement of data over time. It mainly describes if the data has a gradual upward or downward general slope.

III.3.2.2 Seasonality

Many time series present a certain periodicity, let it be annual, monthly or weekly… We will apply this analysis to our case and deduce the general variations of data. These elements of seasonality are easy to detect and can be determined explicitly, but can also be eliminated from the data so to de-seasonalize the series.

III.3.2.3 Random component

Once the previous components are identified, and after having eliminated them, some values are left. The latter are random values. We can analyse these values to determine what type of random behaviour they show, following certain pre-existing models.

III.3.3 Analysis of the Irradiance time series

In the case of our time series, in order to decide which forecasting method should be implemented, we will first analyse the past data. First step is to plot the past 12 years of daily data on a graph:

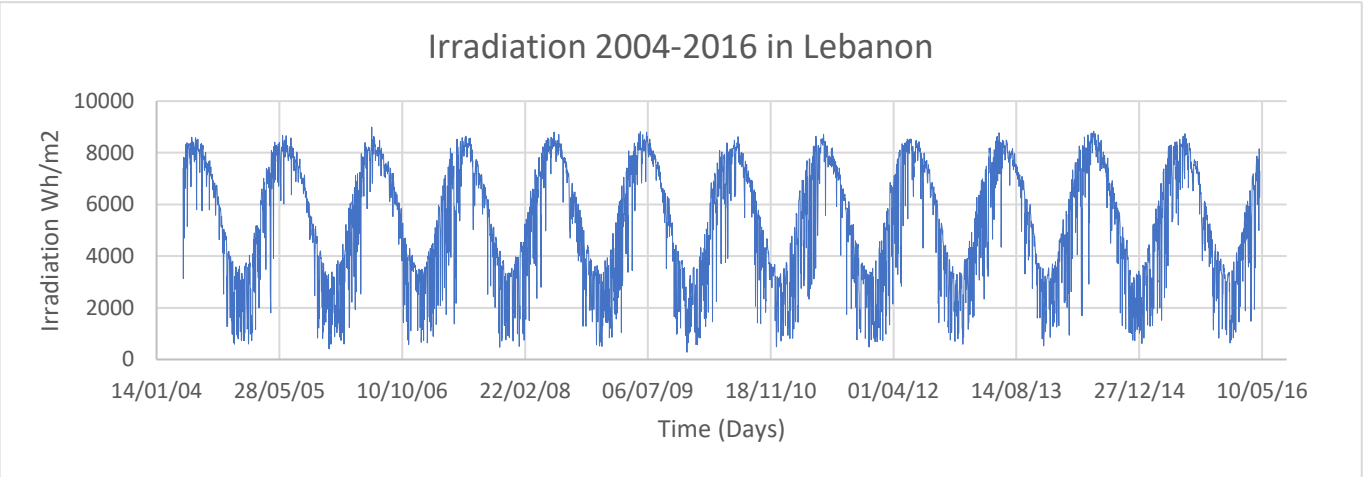

Figure 13: Evolution of the irradiation with time on a two-months range

We can then verify the parameters described before. We observe that this time series doesn't present any trend as the irradiation stays between 0 and 9000 Wh/m2. Moreover, we can notice a certain seasonality of one year. Which means that a same pattern will be repeated every year. This hypothesis makes perfect sense, as the irradiance must have about the same value depending on the seasons: a higher irradiance value for summer, a lower value for winter, and an intermediate one for spring and autumn. We also notice that summer is the moment when there are less variations in the irradiance, compared to winter where very high variations exist.

We can also see some random points that do not follow the general shape of the data. Which is normal, and we should not suppress this data as it will give us this randomness in our future forecasting process.

Naturally, as our time series presents no trends and is subject to some random errors, we can use the Simple Average forecasting method to predict the future values.

To be able to have two distinct forecasts and compare them, we can also consider an Exponential forecasting method to use the strength of the last recorded data compared with the past one. And as our time series does not present any trend, but have a very strong seasonality, the Triple Exponential Smoothing is the method that fits the best our time series.

III.4 Needs for each scale

In the framework of this thesis, we will be considering two scales: Daily Scale Monthly Horizon (DSMH) and Hourly Scale Daily Horizon (HSDH). In each one of the scales, in order to run the Energy Management System optimizing the cost function, a certain number of parameters should be defined.

Concerning the DSMH, the two main data are needed: 1-month ahead forecast for the power generated by the photovoltaic generator, and temperature.

As for the HSDH scale, we will need 1-day ahead forecast for the power generated by the photovoltaic generator, and temperature.

SODA database Helioclim provides us with the Irradiance and Temperature forecast for the HSDH scale. Unfortunately, this data is not provided for the DSMH scale. In this case, we will do our own computation of the Irradiance forecast using both the Simple Average and the Triple Exponential methods and use a yearly Temperature forecast that is provided by the database.

III.5 Results, Errors and comparison

III.5.1 Types of errors

Once we will use both forecasting methods, we have to decide which one will be most accurate. To do so, we need a criterion to evaluate the exactitude of each method. By exactitude we mean how well does the forecast correspond to the actual real values. For a time series, a common method is to use past data to forecast a more recent past data.

The difference between a forecast value and the reality is called a forecast error. We usually use the following equations to compute these errors [29]:

- Mean error

$$ME = \frac{\sum_{i=1}^{n} e_i}{n}$$

- Mean absolute Deviation

$$MAD = \frac{\sum_{i=1}^{n} |e_i|}{n}$$

- Mean square error

$$MSE = \frac{\sum_{i=1}^{n} e_i^2}{n}$$

- Standard deviation of the errors

$$SDE = \sqrt{\frac{\sum_{i=1}^{n} e_i^2}{n-1}}$$

- Percent Error

$$PE_t = \frac{X_t - F_t}{X_t} \times 100$$

- Mean Percent Error

$$MPE = \frac{\sum_{i=1}^{n} PE_t}{n}$$

- Mean Absolute Percent Error

$$MAPE = \frac{\sum_{i=1}^{n} |PE_t|}{n}$$

We are going to consider all these errors in order to compare the two methods we are using.

III.5.2 Simple Average Method

The Simple Average method, as discussed before consists in computation of the unweighted average of the values of the past data, and to assign this value to the forecast data. In our case, we averaged the irradiation from 2004 to 2016 to determine the values for 2017.

We can plot both forecast and real data in a graphic and compare the general shape:

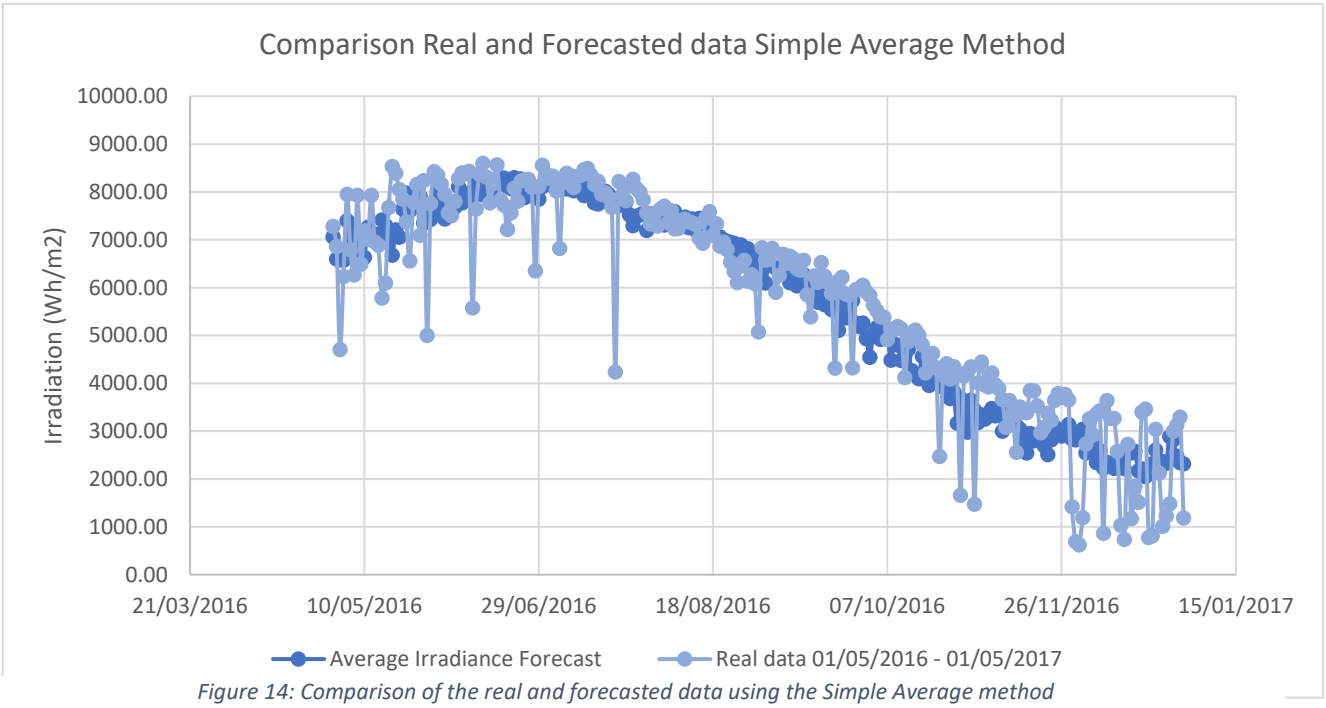

Figure 14: Comparison of the real and forecasted data using the Simple Average method

The first observation is that the forecast follows the real data shape very accurately. Obviously, as the forecast uses an average method, the forecast curve is smoother, and does not present random errors as the real data does.

We also compute the different errors, and we obtain the following results:

Errors		
Mean Error	53.19	
Mean Absolute Deviation	782.26	
Mean Square Error	1021878.79	
Standard deviation of the errors	7.30	
Mean Percent Error	-9.35	%
Mean Absolute Percent Error	26.33	%

Table 3: Errors generated by the Simple Average method

These values will make more sense once we compare them with the errors from the second forecasting method.

III.5.3 Triple Exponential Smoothing Method

The Exponential Smoothing Method considers that the recent data has more weight in the computation of the future data than the past one. This weight is applied exponentially in this method. We wrote a Matlab code that computes the forecast values based on the past ones from 2004 [Annex 5].

Concerning the Triple Exponential Smoothing Method, after the algorithm initialization, 3 parameters have to be initialized as well: $\alpha, \beta \; and \; \gamma$. Using the literature [26] [30] [31], we have the following conditions on these constants:

- α represents the level, it should range in $\alpha \epsilon [0.01 \; ; 0.30]$
- β represents the trend, it usually ranges $\beta \epsilon [0.01 \; ; 0.176]$. In our case, as there is almost no trend, β should be close to zero
- γ represents the seasonality, it usually ranges $\gamma \epsilon [0.05 \; ; 0.50]$.

We had to run a certain amount of experiments in order to find the values of α, β and γ that minimizes the errors. The final values that gave us the minimum prevision error were:

$$\begin{cases} \alpha = 0.150 \\ \beta = 0.005 \\ \gamma = 0.050 \end{cases}$$

The same errors are calculated, so we can compare them with the Simple Average Method errors.

Errors		
Mean Error	4.79	
Mean Absolute Deviation	799.31	
Mean Square Error	1097547.67	
Standard deviation of the errors	2.19	
Mean Percent Error	-10.03	%
Mean Absolute Percent Error	26.76	%

Table 4: Errors generated by the Triple Exponential Smoothing method

We also need to check the error generated by each method. We then plot these values as well as the real data.

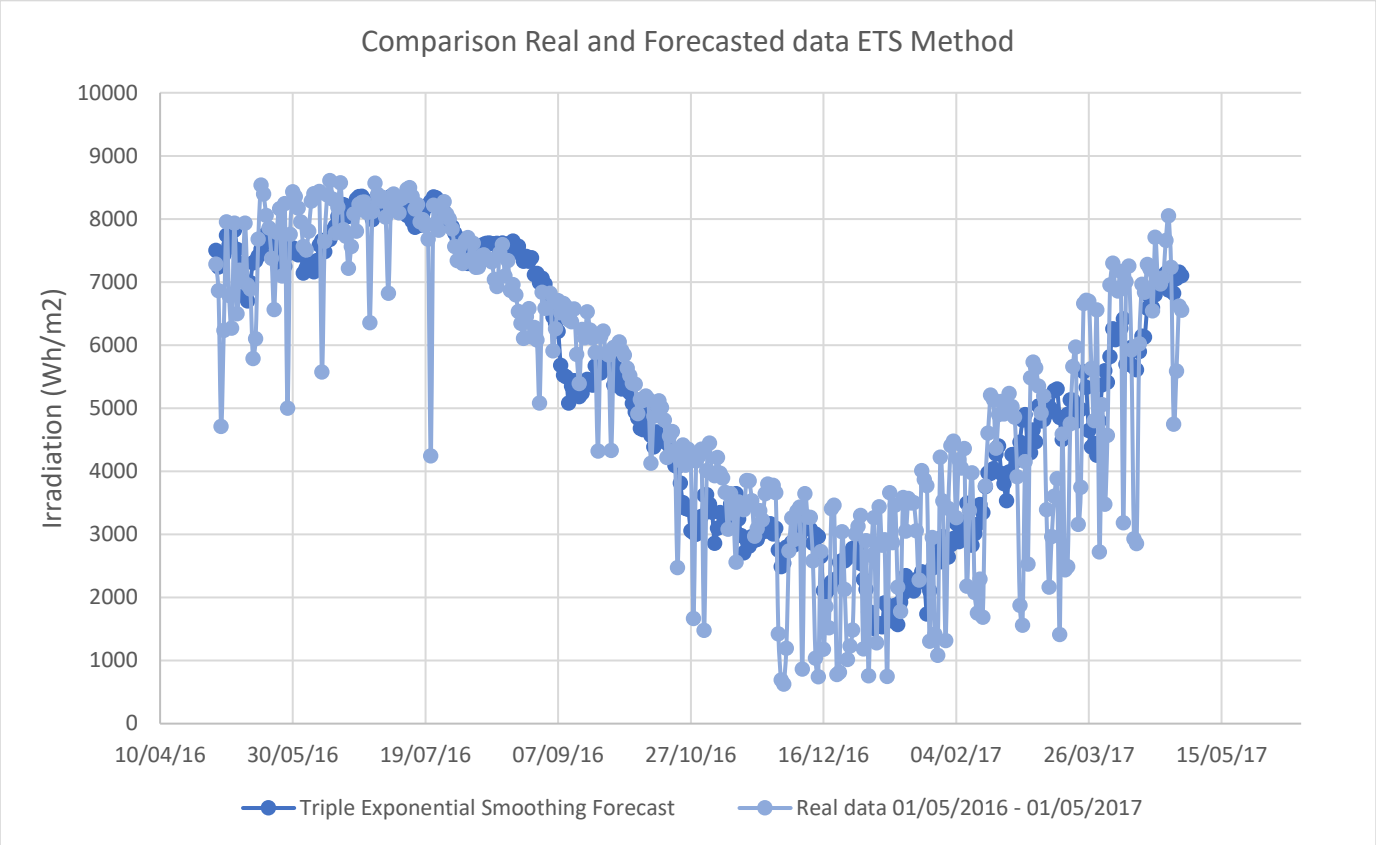

Figure 15: Comparison of the real and forecasted data using the ETS method

The final comparison of the errors can be described as follows:

Errors	Simple Average		Exponential smoothing	
Mean Error	53.19		4.79	
Mean Absolute Deviation	782.26		799.31	
Mean Square Error	1021878.79		1097547.67	
Standard deviation of the errors	7.3		2.19	
Mean Percent Error	-9.35	%	-10.03	%
Mean Absolute Percent Error	26.33	%	26.76	%

Table 5: Comparison between Simple Average and Triple Exponential Smoothing using different errors definitions

III.6 Final decision

To compare both methods, we verify the different types of errors and we notice that both methods have more or less the same accuracy. The difference lies in some values that differ slightly. However, we can observe that the Simple Average method seems to be a little more accurate. Which makes sense, because as we mentioned before, the Simple Average method implies that the values of the series are in equilibrium around a constant value (the mean of the series), when the series is subject to random errors. This is exactly the case of the data series of weather forecast.

Finally, the Simple Average method is a faster method in the execution process than the Triple Exponential. The time parameter also gives the preference to the Simple Average method over the Triple Exponential Smoothing. Consequently, we will use the Simple Average method for the rest of our forecasting calculations.

IV. Rolling Horizon Method

IV.1 Definition and motivation

The Rolling Horizon approach is a reactive scheduling method [8][9][16], that solves iteratively the deterministic problem of the forecast by moving forward the forecasting horizon in every iteration. Once one value of a parameter to be forecasted is known, the status of the system is updated, and the optimal schedule for the new resulting scenario is decided. This approach considers two elements: A prediction horizon, during which the value of the parameter is known considering a possible error, and a control horizon, which decides to change the actual values of the parameter on the next prediction horizon in the case these values are to be changed.

The iterative aspect of this approach allows to update the forecasted value in order to minimized the error considered depending on the current data available. The main goal of the Rolling Horizon approach is that it solves the uncertainty concerning the values needed and hence decreases the errors related to them [18].

The following figure explains this approach: each step, we roll the time horizon by one discretization time interval. Moreover, the values of the parameters to be forecasted are determined through a procedure that minimizes the errors between the predicted output and the reference real value. The procedure is repeated successively.

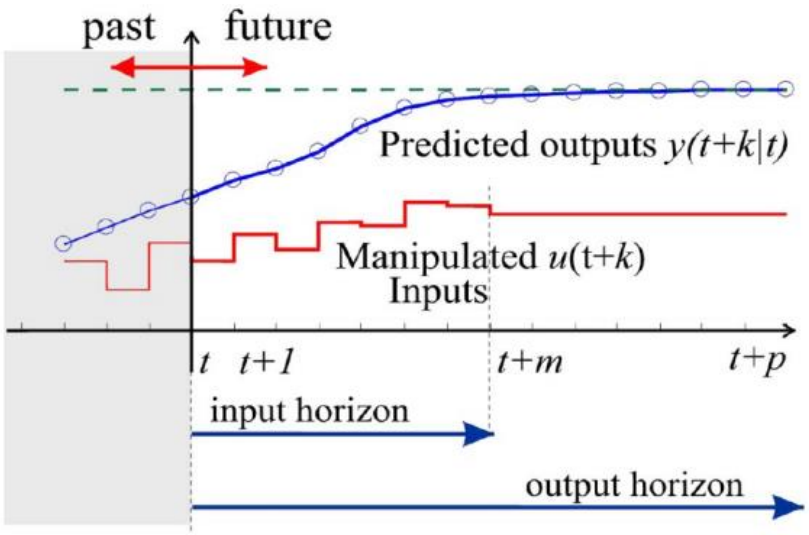

Figure 16: A typical Rolling Horizon approach [9]

In our case, we will use the Rolling Horizon to forecast the Photovoltaic generation and the Load demand, for both time scales.

For the DSMH, the prediction horizon will be a month, and the discretization time is one day. As for the HSDH, the prediction horizon is one day and the discretization time is one hour. Moreover, our Rolling Horizon will function as follows: We will first launch 23 iterations of the rolling of the HSDH, then the 24th iteration will be a DSMH rolling. The scheme below describes the whole procedure:

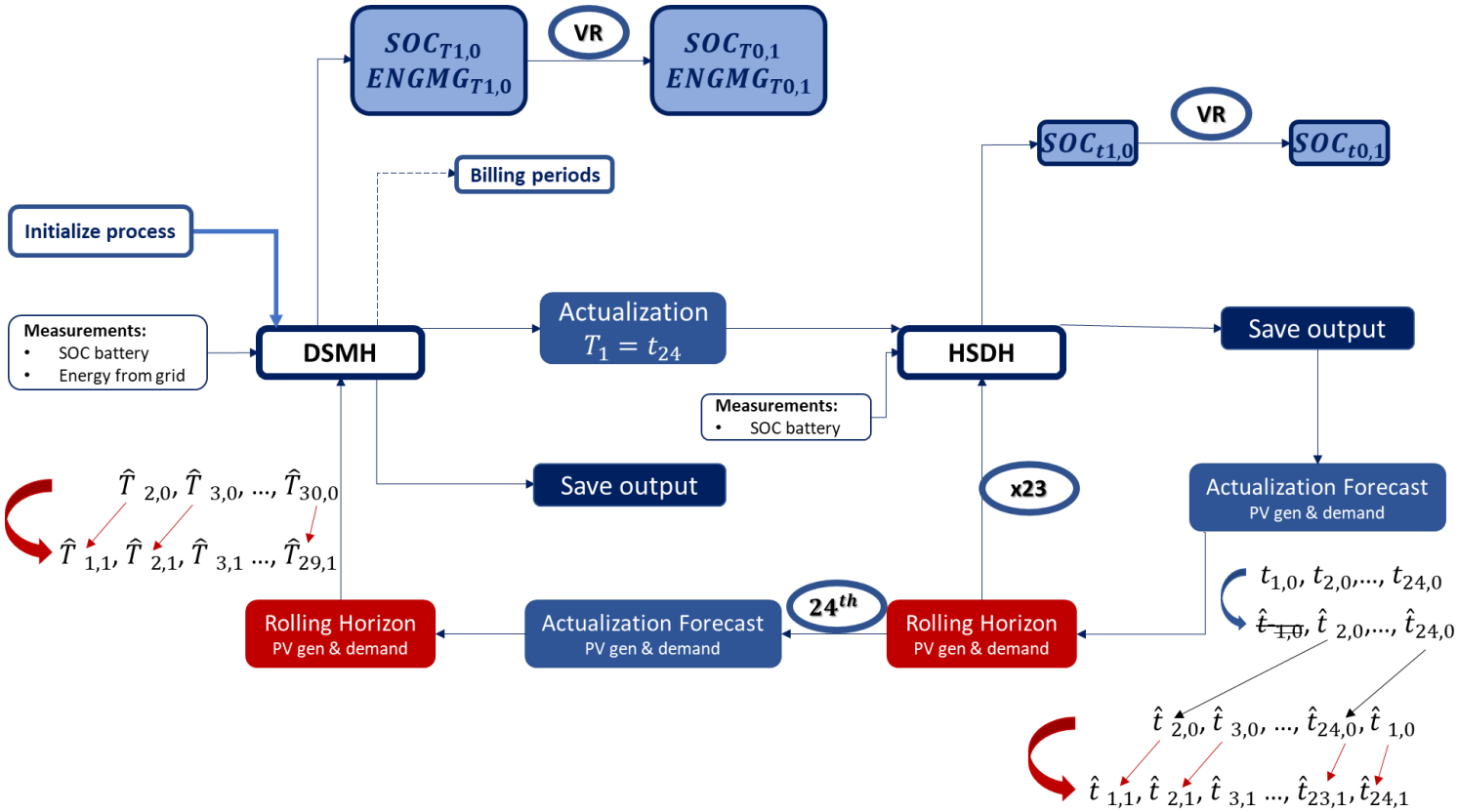

Figure 17: Rolling Horizon Procedure for the Forecast of PV generation and Energy demand

IV.2 Implementation

The figure above describes the general working procedure of the Rolling Horizon approach applied to our case. We will first explain the process on the HSDH scale: the HSDH system receives as input the State Of Charge (SOC) of the battery. We mention that for the DSMH, another data is introduced too, which is the Energy from the grid.

Once the SOC data is introduced in the system, it generates and saves the output. From one side, it will be used to graphically represent this information, but we will also use it to define the forecast values for Photovoltaic generation and demand.

The process goes as follow: First, the forecast data is actualized. In the case of the HSDH scale, this data comes from the SODA database Helioclim that we presented before. We then possess $\hat{t}_{1,0}$, $\hat{t}_{2,0}$,…, $\hat{t}_{24,0}$. We represented the forecast values using $\hat{t}$.

The indexes have the following meaning: The first index represents the order of the data, and the second index represents the number of the iteration. $\hat{t}_{1,1}$ is the first forecast value of the first Rolling Horizon iteration, $\hat{t}_{2,1}$ is the second forecast value of the first Rolling Horizon iteration, $\hat{t}_{1,2}$ represents the first forecast value of the second Rolling Horizon iteration.

The "first forecast value" means that it is the value that will actually be used in the cost optimization algorithm. All the other forecast values can be subject to a change (increase or decrease), depending on the future iterations forecast values. In the case of SODA database Helioclim, the actualization of the data is done every 15min. Hence, using the Rolling Horizon approach will enable us to take advantage of this fast time of actualization. Which we couldn't if we did not use this method.

Next step is the Rolling Horizon itself, as we can see on the scheme (represented in red), the value of the forecasting named $\hat{t}_{2,0}$ becomes the new value of the next forecast, i.e $\hat{t}_{1,1}$.

In a nutshell, every time we actualize the forecast for the next 24 hours (in the HSDH scale), and the value of the next hour **h** is stored on the first cell of the row of forecast values. Then, this first value will be the one used in the algorithm. Finally, we actualize the forecast again, and the forecast value of **h+1** is stored on that first cell.

Of course, the row is composed of 24 cells, and the 24 cells are always full as everytime we empty the first cell to put the value of the next hour, all the values climb up and the last cell contains the first hour of the next day, etc…

The following scheme represents how the Rolling Horizon functions from the row of cells point of view:

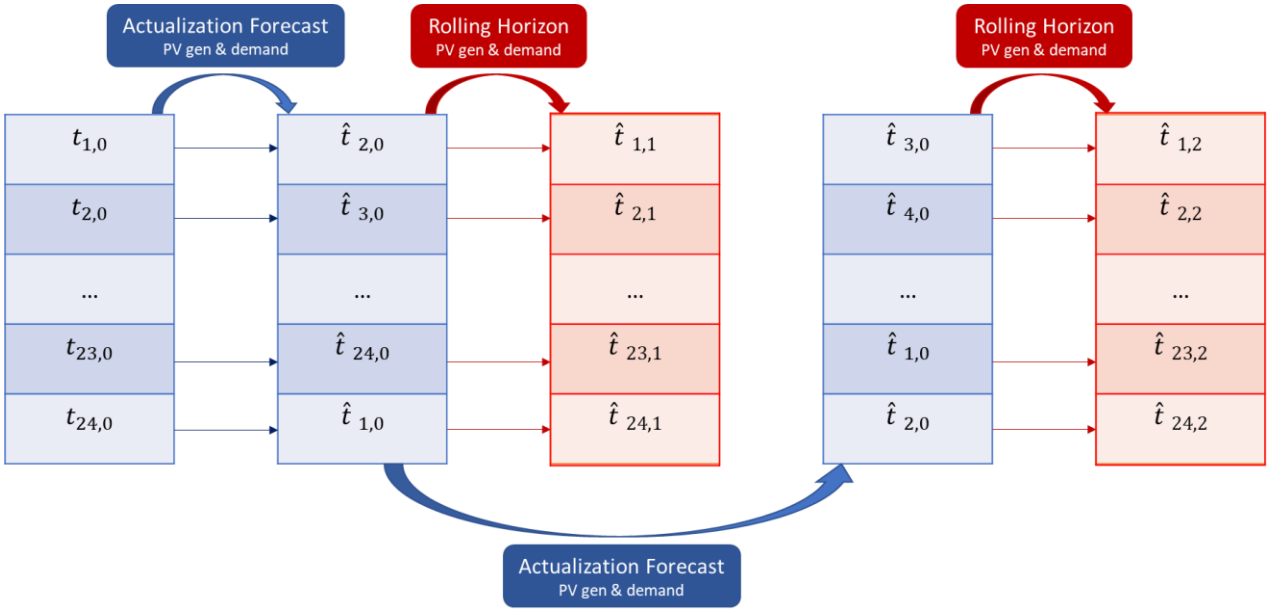

Figure 18: Representation of the succession of Actualization of Forecast and Rolling Horizon

The large blue arrow represents the Actualization of Forecast every discretization time, while the large red one represents the Rolling Horizon process on this forecast values.

As for the thin arrows, they have the following meaning:

The blue one shows the change in the value taking place at the n-position of the column of data. As explained before, the 1st cell for example will always be filled with the value of the forecast that will be used in the next iteration, i.e at h+1 in the case of the HSDH. The next cells contain the rest of the forecast values that will have as a purpose to have an idea about the future variations of the data.

The thin red arrow represents the Rolling Horizon method. The first one, for example, shows that the forecast value $\hat{t}_{2,0}$ -that is the forecast value of the second hour of the day and first iteration of the Rolling Horizon-, will take the first position in the row of the forecast values. In other words, in the next iteration, the value $\hat{t}_{2,0}$ will be used to represent the second hour of the day.

Then, the next step is represented by the second large blue arrow. The new forecast values, given by the SODA database Helioclim in the HSDH scale, are stored in this Forecast column (Blue). Of course, the first and second hours having passed already, no forecast exists for these values, we hence start at $\hat{t}_{3,0}$.

Again, the Rolling Horizon operates, it is represented by the large red arrow. As it can be seen, in the position 1 of the column, for the iteration 2 of the Rolling Horizon ($\hat{t}_{1,2}$), we fill in the latest forecast value of the 3rd hour. This is represented with the thin red arrow.

The procedure continues again and again until the end of the day (hour 23), after which, the larger loop will be followed: The 24th loop will be on the DSMH scale.

As mentioned before, the forecast for the photovoltaic generation and demand for the DSMH scale are handled differently. We will be computing directly using the method described in the previous section. However, the general working principle of the Rolling Horizon does not change depending on the source of the data as this forecast values are only inputs. The only step we should not miss is to make sure we have actualized the forecast every discretization time interval. Which will enable a smooth rolling of the data.

Concerning the 24th iteration, the process is very similar, the new actualized data is stored on the first cell of the Actualized Forecast DSMH column named here $\hat{T}_{2,0}$, then it will be stored for the first iteration of the Rolling Horizon in the $\hat{T}_{1,1}$. -We used capital T to distinguish the DSMH scale from the HSDH-.

In the case of Lebanon, we also have to take into consideration the tariffs applied for the energy used from the grid. The system is based on a graded monthly tariff. Which means that the energy price is constant for a consumption below a certain level, and each level has a different price. Hence one should consider the consumption day by day to make sure not to surpass the necessary consumption to stay in the wanted grade for the month. It is represented in the scheme by the “Billing periods” output.

This fact influences the DSMH scale: We have two main inputs to the system: The SOC of the battery but also the Energy taken from the grid.

The SOC of the battery is represented as follows:

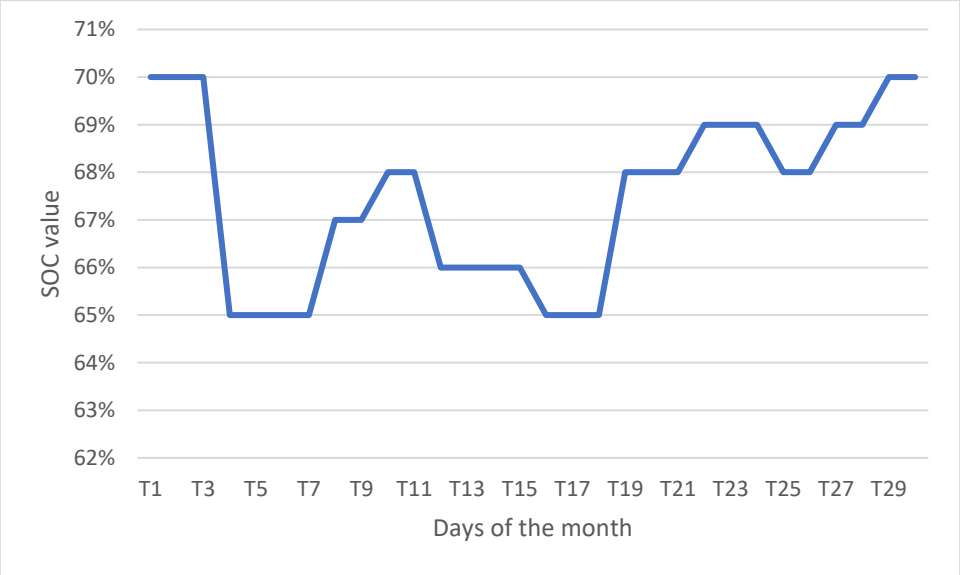

Figure 19: Variations of the SOC value

Its value (which ranges between 0 and 1 in theory), is assumed to be initialized at 70% (0.7), we also define that the upper limit is 70%. Then, with time, this value will vary around this value in a certain interval. We hence defined the SOC error, which represents the percentage of the SOC with which the value of the SOC varies.

In order to test the ability of the EMS to manage the variations of the SOC, this SOC value will be randomly simulated using different values of SOC error so to analyze its influence.

For a SOC error of 1% for example, we define the SOC value as follow:

$$SOC(T_i) = SOC(T_1) \times (1 + ((R - 0.5) \times 0.02))$$

Where:

$SOC(T_i)$ is the value of the SOC at a time T_i

$SOC(T_1)$ is the value of the SOC at the initial time T_1

R is a random number in the range [0;1]

This definition makes sense when knowing our objective: obtaining a value of the SOC with an error from the initial value of 1% in our example.

By definition,

$$0 \leq R \leq 1$$

Hence

$$-0.5 \leq R - 0.5 \leq 0.5$$

$$-0.01 \leq (R - 0.5) \times 0.02 \leq 0.01$$

Finally,

$$-1\% \leq (R - 0.5) \times 0.02 \leq 1\%$$

Naturally, we can represent a SOC error of any percentage using a similar equation.

IV.3 Results, comparison with no Rolling Horizon

We finally apply the Rolling Horizon to our system and we track the evolution of the Photovoltaics generated. We measured this data using the Rolling Horizon and plotted it from 07:40 to 12:28. This is the period where the information is the most critical for our needs.

Our extractions, actualization of the forecast and RH method are done hourly in the HSDH scale as the discretization time is one hour. We plot some of these data with the purpose of comparison between the first and last extractions of the day.

Obviously the first extraction of the day will represent the forecast with the highest error as we still don't know much about how the weather is going to be. The more we go through the day, the more information we have concerning the possible evolution of the weather and hence the photovoltaic generation. Consequently, the errors are minimized by the end of the day.

The main point from this information is that the last forecast values of the day represent the *reality*: In fact, at 11:00 for example, all the irradiation data given by the database after 11:00 is a forecast. However, the data given before 11:00 is a measurement. Which means the real data.

Now, we can analyse our plot:

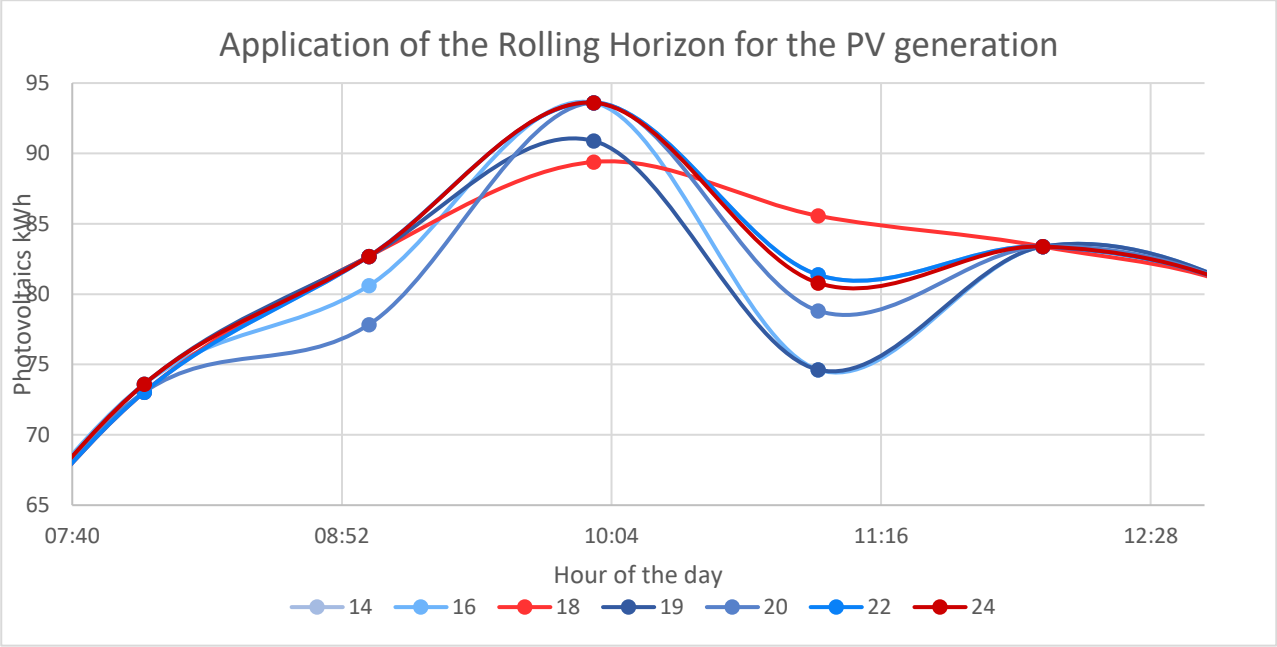

Figure 20: Example of the application of the Rolling Horizon on a sample

The red curve corresponds to the last Photovoltaic generation of the day, which also means the real photovoltaic generation. The other curves represent other extractions at different moments (14:00, 16:00, 18:00 and so on). We can see the evolution of the forecasts with time: Photovoltaics values vary randomly around the final value.

In addition, one can verify the benefits of using the Rolling Horizon and compare the photovoltaic generation forecast with and without Rolling Horizon. We plot the two results in the following graph:

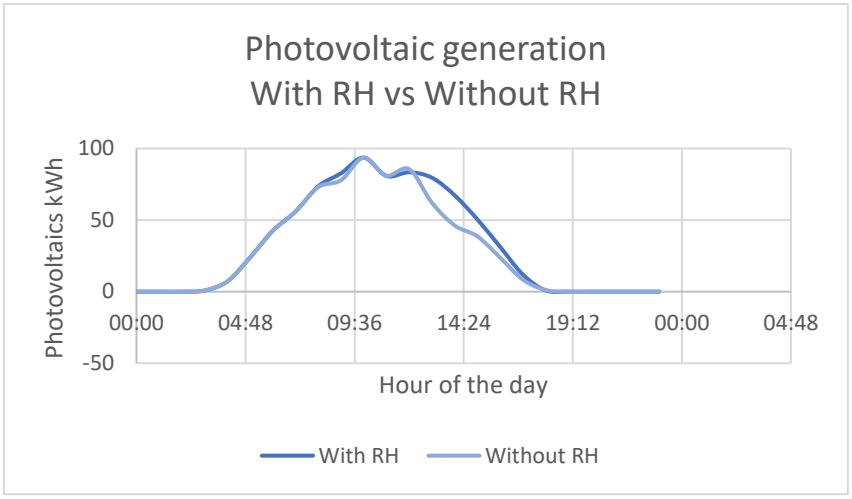

Figure 21: Comparison of photovoltaic generation with and without the Rolling Horizon approach

We notice that for the first hours of the day, the two methods show the same results. Which seems accurate, as the error of prediction of the first hours of the day are very low even without the Rolling Horizon. However, on the second part of the day, we see that the values differ more. We hence understand the importance of the Rolling Horizon that is keeping track of the newly updated forecast and consequently reducing the error of prediction. The use of this method will give us more accurate results.

We also plot the error between the two methods. We observe again that the error is more present on the second part of the day, which corresponds to the information we gathered from the first graph.

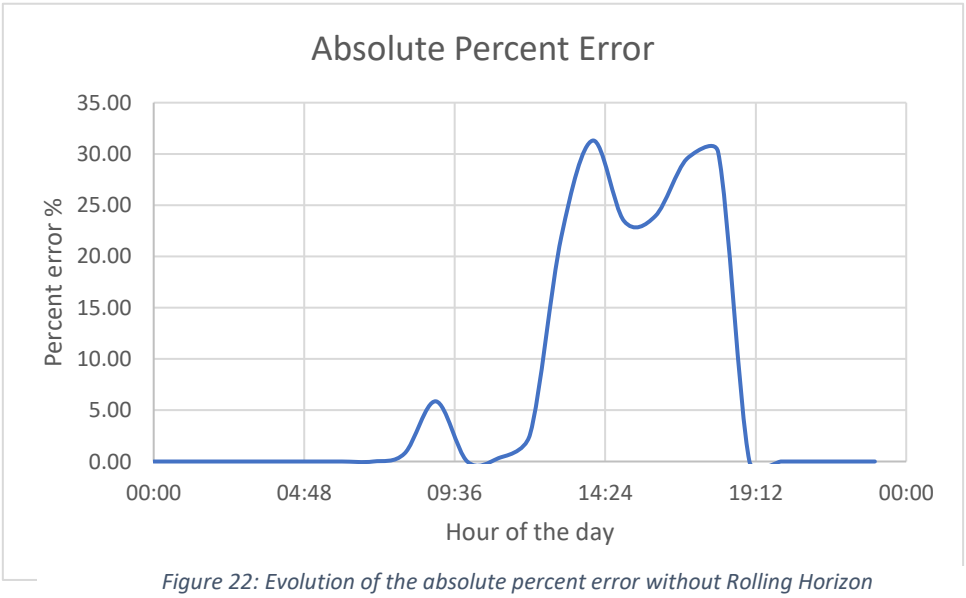

Figure 22: Evolution of the absolute percent error without Rolling Horizon

V. Forecasting errors – Parametric Analysis

V.1 Influence of the SOC error on the cost function

The goal main of the EMS is to provide enough energy for all the demand while minimizing the cost function. It is an optimization problem, and many parameters should be taken into account to determine how this cost function evolves.

One of the main parameters is the SOC of the battery. In fact, the behaviour of the battery affects the storage particularity of the system and consequently the cost function itself.

In order to understand better the influence of the SOC error on the cost function, we performed a parametric analysis. For a range of values of the SOC error, we exploit the optimized cost function computed by the algorithm of the EMS on GAMS (General Algebraic Modelling System) [17].

We obtain the following data:

SOC error	Cost ft1	Cost ft2	Cost ft3
1%	35324006.26	35324006.26	35324006.26
5%	34863096.72	35028922.86	34922068.7
10%	35264068.09	35578533.33	35458366.52
20%	35856768.12	36226612.33	36461225.65

Table 6: Evolution of the cost function with the SOC error of the battery

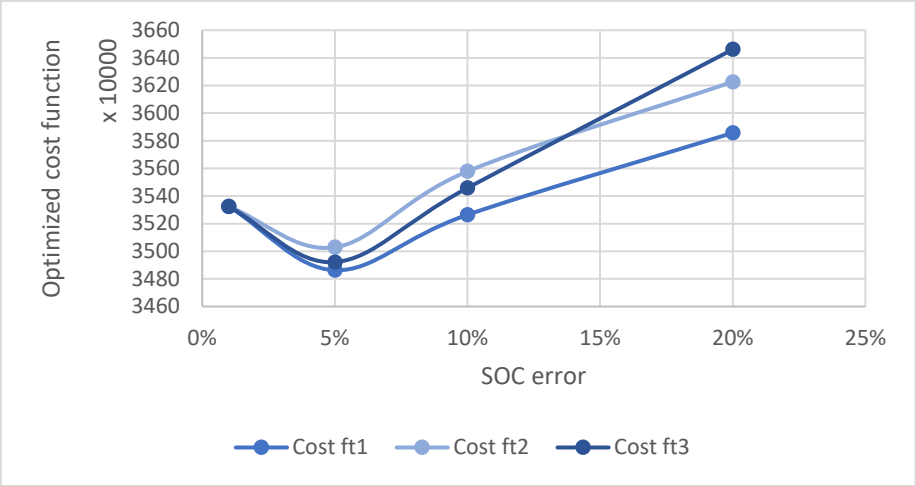

Figure 23: Evolution of the cost functions for 4 different values of the SOC error

We notice that the values have a same general behaviour, but we also notice that for lower values of the SOC error, the values of the cost function are close to a same value. On the other hand, as the values of the SOC error are higher, the values of the cost function are dispersed. The small SOC error represents a stable moment of the year -around summer- when, as we mentioned before, the prediction error if the smallest. On the opposite, a high SOC error represents the non-stable moment of the year -around winter- when the difference between the real and the forecast value is higher, which means the prediction error is higher.

From this experiment, we conclude that when the forecasting is done during a stable period, the cost function has a constant value and when the period is less stable, the cost function very dispersed values. Which makes sense as the more stable the moment is, the less the error in prediction there is and the better the scheduling for the next period will be. Consequently, the more stable the value of the cost function will be.

We also compute the average of all the repeated experiments with these 4 values of the SOC error in order to smooth the data. We obtain the following:

SOC error	Average
1%	35324006
5%	34938029
10%	35433656
20%	36181535

Table 7: Evolution of the average cost function with the SOC error of the battery

We also plot the graph:

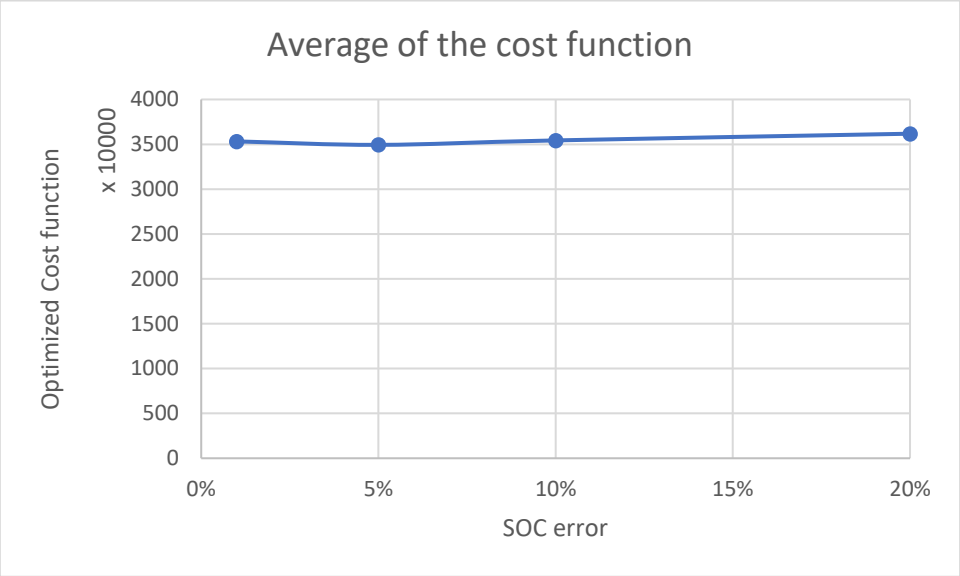

Figure 24: Evolution of the average of the cost function for 4 different values of the SOC error

We notice that the value of the cost function is constant in average. Hence, even with high variations of the SOC error, i.e. variations of the moments of the year during which the prediction is done, the cost function does not vary much. We can then conclude about the robustness of our system, since with a highly dispersed input (SOC error), the output is almost constant.

V.2 Influence of the demand on the cost function

Another parameter that should be taken into account is the demand. Naturally, as the demand varies, the energy generation must vary and consequently, the cost function varies. We perform a parametric analysis on the demand for different values, and retrieve data concerning the corresponding cost function from the EMS simulated by the GAMS algorithm [17].

We take the daily energy consumption profile in Lebanon that has the following overall shape:

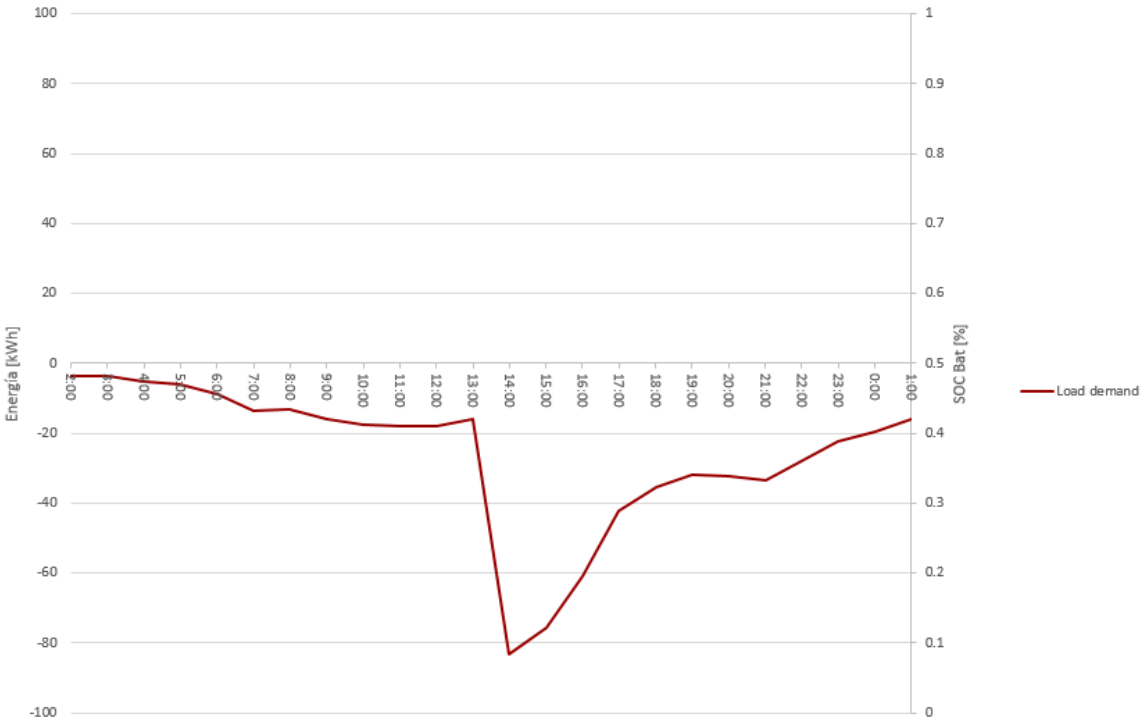

Figure 25: Energy profile for a weekday in Lebanon

This state of the consumption the standard situation of the demand. Then, we define the fraction of the energy demand, the coefficient that multiplies each one of the values of the profile.

We then compute the cost function related to each consumption profile. We obtain the following:

Fraction of energy demand	Cost function
0.5	1582.36
1	35324006.26
1.2	1471301390
1.3	2128302897
1.5	9992120310

Table 8: Evolution of the cost function with the demand

We also plot the evolution of the cost function with respect to the energy demand. We observe that the cost function increases with an increasing demand. We also notice a peak: The saturation point.

We can supply more or less loads with higher and higher increments, but at the saturation point, the devices in the grid cannot supply anymore because they reached their limit. There is a penalty fee when loads are not supplied. And the more non-supplied loads there are, the higher the penalty is. Until the point when the cost becomes really high.

When the limit capability to increase the demand is reached, the system needs to be re-dimensioned.

In this case, the saturation point lies at a demand factor of 1.3.

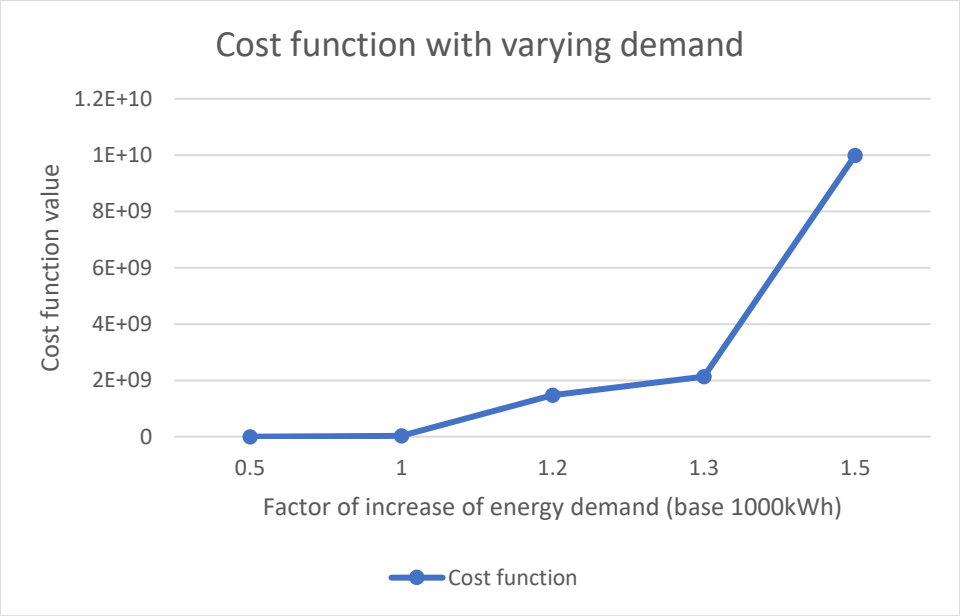

Figure 26: Influence of the demand on the cost function

VI. Exploitation of the tool: Cases of study

Once we defined the influence of different parameters on the cost function of this system, we can test it on some situations and understand the behaviour depending on some parameters. Two main variables can be varied: The monthly blackouts and the grid tariff ranges.

VI.1 Grid energy Tariffs

As mentioned before, the grid tariffs in Lebanon have a special policy based on a graded monthly tariff, where depending on the quantity of energy consumed, the price depends on the energy levels defined beforehand.

In this experiment, we run simulations with different Grid tariffs. The table below summarizes the Grid tariffs considered:

	Interval upper energy level				
	100	**300**	**400**	**500**	**>500**
Tariff range 1	7	11	16	24	40
Tariff range 2	35	55	80	120	200
Tariff range 3	70	110	160	240	400
Tariff range 4	140	220	320	480	800

Table 9: Daily Tariff of Grid energy depending on the upper energy level interval

We then compute the cost function associated to each tariff range, and compare them. The plot is in the figure below:

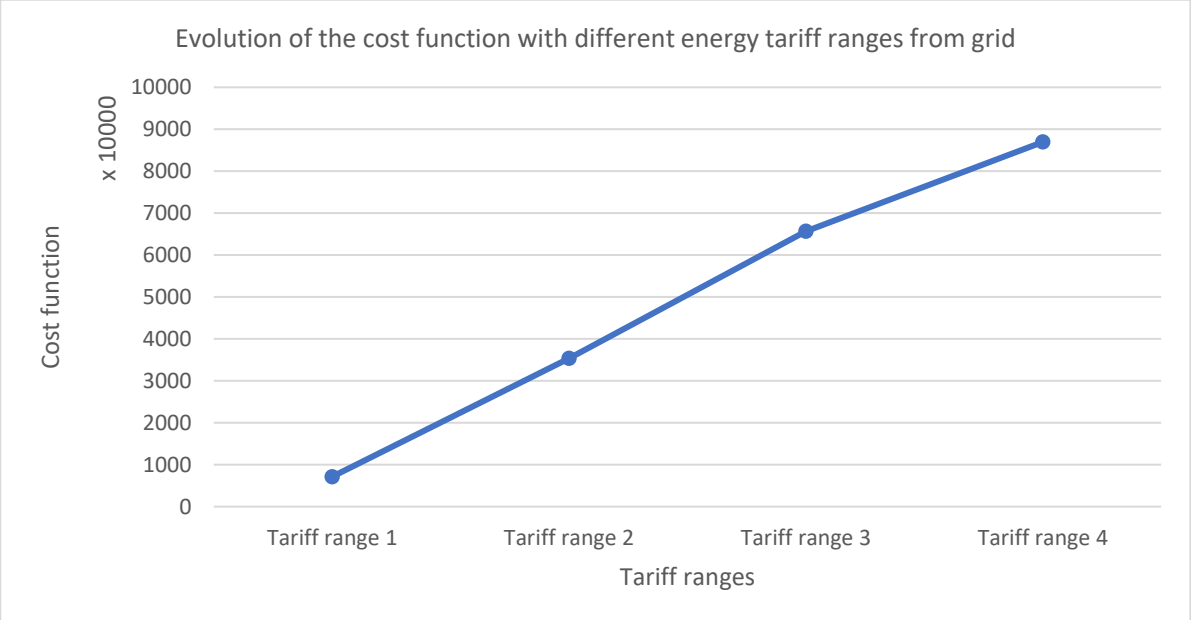

Figure 27: Evolution of the cost function value depending on the tariff ranges mentioned before

Corresponding to the following values:

Tariff Range	Cost function
Tariff range 1	7128922
Tariff range 2	35324006
Tariff range 3	65624052
Tariff range 4	86937825

Table 10: Evolution of the cost function with the different Tariff ranges

We notice an increasing evolution of the cost function, which makes sense as the higher the tariff range, the higher the final cost function for a same energy consumption.

Moreover, we can point out the difference in the slopes of evolution between the different tariff ranges. In fact, the first two points correspond to a very low-priced consumption, hence the cost function is very low. The third point have a higher slope. It corresponds to the normal consumption tariff range and the cost function varies between different values. Finally, the last point corresponds to a very high-priced tariff range, and consequently the cost function is much higher.

The cost function is then influenced by the energy tariff ranges.

VI.2 Monthly Blackouts

Another parameter that can be tested is the blackouts. In the case of Lebanon, the grid blackouts are programmed in advance on a month horizon. The EMS, with this information provided, can take it into consideration in the scheduling of the next operation of the devices.

We implement the following example to visualize the impact of the blackouts on the system. We will consider a situation where two blackouts are programmed during the day. One from 07:00 to 09:00, and the other one from 19:00 to 20:00.

The Model Predictive Control coupled with the Rolling Horizon method gives us the following outputs:

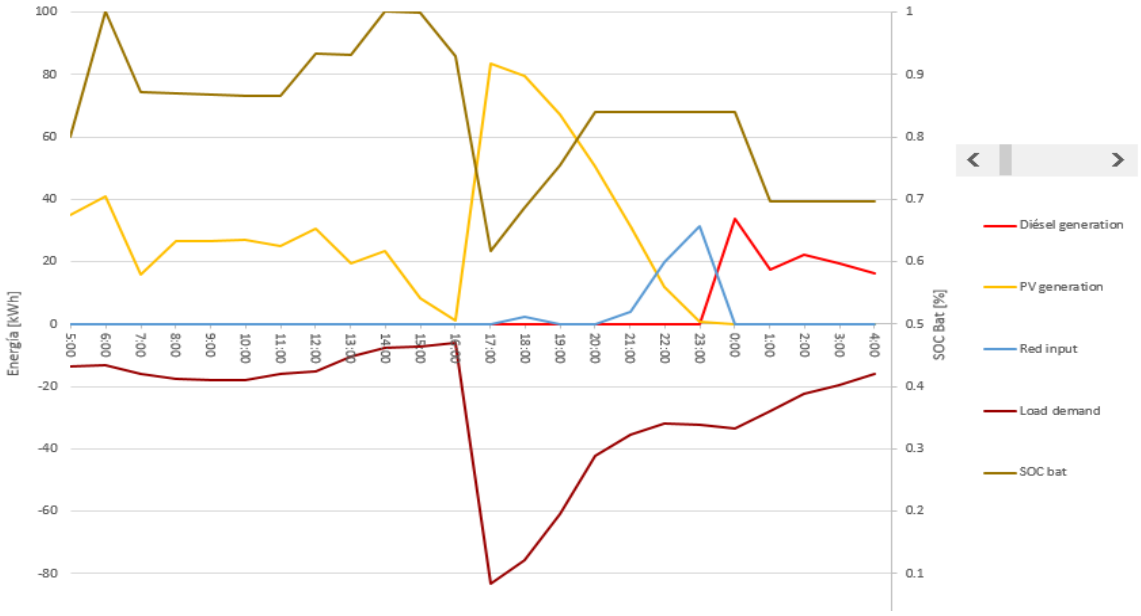

Figure 28: Evolution of the energy exchanges and SOC of the battery for a programmed blackout

On this figure, we can see the evolution of 5 parameters: The Photovoltaic generation (Yellow), the Diesel generation (Red), the Red input (Blue), the demand from the loads (Bordeaux) and the SOC of the battery (Brown).

At 05:00, the prediction is as follows: it is expected that from 06:00, the network will use the battery energy, we then notice a drop in the SOC from 06:00 to 07:00. Then, the Photovoltaic generation is available from 07:00 to 08:00 for a slightly increased consumption (Bordeaux curve), and a constant SOC as we don't use the battery at that moment. From 08:00 to 11:00, the system keeps using the Photovoltaic energy as it is available and sufficient for the demand. From 11:00 to 12:00, there is an increased production of the Photovoltaic energy that is used to charge the battery (SOC increases).

From 12:00 to 13:00, the PV generation and the demand drop, so the battery cannot be charged anymore. Another peak of PV generation associated with a very low demand enables the full charging of the battery.

From 16:00, there is an important drop of the PV generation and consequently a use of the battery. Then, a peak of the PV generation that coincides with a high demand from the loads from 16:00 to 19:00. We observe a small use of the grid energy from 17:00 to 18:00 to help the system with supplying all the demand. After that, the blackout from 19:00 to 20:00 appears with an important demand that is compensated by the PV generation.

Once the PV generation is not enough, by 20:00, the grid input is used then, later on the diesel generation is used (from 23:00) with the battery supply.

We can then notice that with this system, the blackout is foreseen and handled beforehand. And with a monthly horizon blackout data, all shortages can be avoided with this MPC coupled with the Rolling Horizon.

VII. Conclusions and future development

The challenge presented by this work suggested the use of a Model Predictive Control (MPC) on an Energy Management algorithm with the goal to minimize the cost function of a renewable-based microgrid network for an extended horizon of one month. This MPC provides an online real-time scheduling of the generation units considering the forecast of the renewable resources (Photovoltaic generation). A Rolling Horizon approach has also been introduced to reduce the prediction error.

The novelty of this approach is to consider two time scales: daily scale with monthly horizon and hourly scale with daily horizon. This method enables a faster and less consuming process for the energy management. For each scale, a model is defined, and the forecast data for the photovoltaic generation and the load demand is needed.

The access to this data is done differently: The hourly forecast of photovoltaic generation will be extracted automatically from an online database. The daily forecast has been computed directly comparing Exponential Smoothing and Simple Average methods, being this last one that gave a more accurate forecasting for our time series.

The implementation of the MPC combined with the Rolling Horizon proved to be a feasible approach to run the Energy Management System correctly according to the simulation results.

In the next steps of this work, the proposed EMS can consider lower scales to implement the MPC, such as the 15-minutal or 5-minutal scale, as it will provide even more accurate results. Future research can also focus on the management of the battery lifetime during its operating time.

Bibliography

[1] M. P. Marietta, B. Samaniego, F. Guinjoan, G. Velasco, and R. Piqué, "Integration of a Pb-acid battery management algorithm into optimization control strategies for microgrid systems," pp. 128–134, 2017.

[2] Universitat Politècnica de Catalunya - Barcelona Tech (UPC), "Energy Campus. MED-Solar project," UPC, [Online]. Available: https://campusenergia.upc.edu/en/news/med-solar-more-than-one-year-of-project. [Accessed 22 December 2016].

[3] D. E. Olivares, C. A. Cañizares and M. Kazerani, "A Centralized Optimal Energy Management System for Microgrids," in 2011 IEEE Power and Energy Society General Meeting, San Diego, 2011.s

[4] D. E. Olivares, A. Mehrizi-Sani, A. H. Etemadi, C. A. Cañizares, R. Iravani, M. Karezani, A. H. Hajimiragha, O. Gomis-Bellmunt, M. Saeedifard, R. Palma-Behnke, G. A. Jimenez-Estevez y N. D. Hatziagyriou, «Trends in Microgrid Control,» IEEE Transactions on Smart Grid, pp. 1905-1919, 18 Junio 2014.

[5] M. Marietta, F. Guinjoan, G. Velasco, R. Pique and D. Arcos-Aviles, "Analysis of a strategy of predictive control based on time scales for the management of a connected microgrid," in 23th Annual Seminar on Automation, Industrial Electronics and Instrumentation (SAAEI 2016), Elche - Spain, 2016.

[6] D. Limon, J. M. G. Silva, T. Alamo, and E. F. Camacho, "Improved MPC Design based on Saturating Control Laws," *Eur. J. Control*, no. August 2003, pp. 112–122, 2005.

[7] A. Parisio and L. Glielmo, "Energy Efficient Microgrid Management using MPC," in 2011 50th IEEE Conference on Decision and Control and European Control Conference (CDC-ECC), Orlando, 2011.

[8] M. P. Marietta, M. Graells and J. M. Guerrero, "A Rolling Horizon Rescheduling Strategy for Flexible Energy in a Microgrid," in 2014 IEEE International Energy Conference (ENERGYCON), Cavtat, 2014.

[9] G. M. Kopanos and E. N. Pistikopoulos, "Reactive Scheduling by a Multiparametric Programming Rolling Horizon Framework : A Case of a Network of Combined Heat and Power Units," 2014.

[10] M. Savaghebi, J. M. Guerrero, A. Jalilian, and J. C. Vasquez, "Hierarchical Control Scheme for Voltage Unbalance Compensation in Islanded Microgrids," pp. 3158–3163, 2011.

[11] O. Alrumayh and S. Member, "Model predictive control based home energy management system in smart grid," *Electr. Power Energy Conf. (EPEC), 2015 IEEE*, pp. 152–157, 2015.

[12] The MathWorks, Inc., «MATLAB,» [On line]. Available: https://es.mathworks.com/products/matlab/. [last acces: 15 May 2017].

[13] A. Parisio, C. Wiezorek, T. Kyntaja, J. Elo, and K. H. Johansson, "An MPC-based Energy Management System for multiple residential microgrids," *IEEE Int. Conf. Autom. Sci. Eng.*, vol. 2015–Octob, pp. 7–14, 2015.

[14] S. Raimondi Cominesi, M. Farina, L. Giulioni, B. Picasso, and R. Scattolini, "Two-layer predictive control of a micro-grid including stochastic energy sources," *Proc. Am. Control Conf.*, vol. 2015–July, pp. 918–923, 2015.

[15] Electropaedia (2017). Electricity generation from solar energy. [online] Available at: http://www.mpoweruk.com/solar_power.htm [Last access 25 Jun. 2017].

[16] J. Silvente, G. M. Kopanos, E. N. Pistikopoulos, and A. Espuña, "A rolling horizon optimization framework for the simultaneous energy supply and demand planning in microgrids," *Appl. Energy*, vol. 155, pp. 485–501, 2015.

[17] GAMS Development Corporation, [On line]. Available: http://www.gams.com/. [Last access: 01 July 2017].

[18] R. Palma-Behnke *et al.*, "A microgrid energy management system based on the rolling horizon strategy," *IEEE Trans. Smart Grid*, vol. 4, no. 2, pp. 996–1006, 2013.

[19] A. H. Fathima and K. Palanisamy, "Optimization in microgrids with hybrid energy systems - A review," *Renew. Sustain. Energy Rev.*, vol. 45, pp. 431–446, May 2015.

[20] "Solar Energy Service for Professionals", Soda-pro.com, 2017. [Online]. Available: http://www.soda-pro.com/web-services. [Last access: 25 Jun. 2017].

[21] "HC-3 automatic access - Carpentras", Soda-pro.com, 2017. [Online]. Available: http://www.soda-pro.com/help/helioclim/helioclim-3-automatic-access. [Last access: 22 May 2017].

[22] "MeteoGalicia", Meteogalicia.gal, 2017. [Online]. Available: http://www.meteogalicia.gal/web/index.action. [Accessed: 15 May 2017].

[23] "HC3 Persistence model", Soda-pro.com, 2017. [Online]. Available: http://www.soda-pro.com/soda-products/hc3-current-day#top. [Accessed: 09- Jun- 2017].

[24] A. Tuohy *et al.*, "Solar Forecasting: Methods, Challenges, and Performance," *IEEE Power Energy Mag.*, vol. 13, no. 6, pp. 50–59, 2015.

[25] G. T. H. E. Grid, "PRONÓSTICO DE GENERACIÓN DE ENERGÍA EÓLICA Y SOLAR "

[26] "Single Moving Average", Itl.nist.gov, 2017. [Online]. Available: http://www.itl.nist.gov/div898/handbook/pmc/section4/pmc421.htm. [Last access: 20 Jun 2017].

[27] A. Webster, "Técnicas de Suavización," pp. 381–412, 1998.

[28] M. Ivanovic and V. Kurbalija, "Time series analysis and possible applications," *2016 39th Int. Conv. Inf. Commun. Technol. Electron. Microelectron. MIPRO 2016 - Proc.*, pp. 473–479, 2016.

[29] D. Escribano Mateo, "Gestión de la planificación de la demanda en Henkel Ibérica," pp. 1–83, 2012.

[30] E. Upc, “2.1.3 Medias móviles,” pp. 61–119, 1998.

[31] C. Caplice, "Exponential smoothing: Seasonality", MIT Center for Transportation and Logistics, 2016.

Appendices

[Annex 1] MEDsolar Project presentation

Machrek Energy Development – Solar
Project 00087030

General Information

Short Title:	**MED-Solar**
UNDP Programme/Portfolio:	**Environment & Energy**
Geographic Coverage:	**Lebanon**
Project Status:	**Ongoing**
Start Date:	**01 January 2013**
Expected End Date:	**30 September 2016**
Implementing Agency:	**UNDP (Direct Execution) (UNDP)**
Last Updated:	**01 March 2017**

Classification

MDG Goal:	**7. Ensure environmental sustainability**

Contact Information

Project Manager:	**N/A**
UNDP Portfolio Manager:	**Jihan Seoud**
Address:	**Maarad street, building 287 B, 1st floor Beirut, Lebanon**
Phone:	**+961 1 981 944**
Fax:	**+961 1 981 944**
Website:	**www.undp-cedro.org**
Email:	**info@cedro-undp.org**
Working Hours:	**9:00 am to 5:00 pm**

Donors & Budget

EC	**$1,016,405.00**
Total	**$1,016,405.00**

Target Groups / Beneficiaries

- Industries

Project Details

Background

The ENPI regional energy project aims at the promotion and implementation of innovative technologies and know-how transfer in the field of solar energy, particularly PV systems. In the target countries; Lebanon, Jordan and Palestinian, the weakness of the grid, in terms of blackouts and brownouts, undermines security of supply in critical facilities and in small and medium size industries. For these institutions, existing expensive diesel generators make up for the times that the grid is not present. The introduction of a novel photovoltaic (PV) – national grid – diesel grid architecture is important to be set up so that the commercial sector in the country can begin the integration of PV systems, saving on grid and diesel costs.

Achievements & Expected Resutls

The capacity building and implementation of the projects in Lebanon are completed as follows:
- EMKAN, Rene Mouad Foundation, Tahrir and the American University of Beirut were selected as adequated sites after the development of site selection criteria, reviewing applications and properly commissioned to Beneficiaries.
- Installation and setup of systems.
- Inauguration event for AUB site was held in July 2016.

Issues & Difficulties

Page 1 of 1

[Annex 2] SunTech 300-24/Ve PV panel datasheet

STP305 - 24/Ve
STP300 - 24/Ve
STP295 - 24/Ve
STP290 - 24/Ve

SUNTECH

305 Watt
POLYCRYSTALLINE SOLAR MODULE

Features

High module conversion efficiency
Module efficiency up to 15.7% achieved through advanced cell technology and manufacturing capabilities

Excellent weak light performance
Excellent performance under low light conditions

Positive tolerance
Positive tolerance of up to 5% delivers higher outputs reliablity

Suntech current sorting process
System output maximized by reducing mismatch losses up to 2% with modules sorted & packaged by amperage

Extended wind and snow load tests
Module certified to withstand extreme wind (3800 Pascal) and snow loads (5400 Pascal) *

Withstanding harsh environment
Reliable quality leads to a better sustainability even in harsh environment like desert, farm and coastline

Certifications and standards:
IEC 61215, IEC 61730, conformity to CE

Trust Suntech to Deliver Reliable Performance Over Time

- World-class manufacturer of crystalline silicon photovoltaic modules
- Unrivaled manufacturing capacity and world-class technology
- Rigorous quality control meeting the highest international standards: ISO 9001: 2008, ISO 14001: 2004 and ISO17025: 2005
- Regular independently checked production process from international accredited institute/company
- Tested for harsh environments (salt mist, ammonia corrosion and sand blowing testing: IEC 61701, DIN 50916:1985 T2, DIN EN 60068-2-68)***

Compact and Durable Frame Design

The new compact frame means more modules per package, so it saves your shipping and inventory cost. The rigid and durable hollow chamber guarantees the same long-term and reliable performance.

Industry-leading Warranty based on nominal power

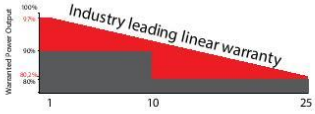

- 97% in the first year, thereafter, for years two (2) through twenty-five (25), 0.7% maximum decrease from MODULE's nominal power output per year, ending with the 80.2% in the 25th year after the defined WARRANTY STARTING DATE.****
- 10-year material and workmanship warranty

IP67 Rated Junction Box

Supports installations in multiple orientations. High reliable performance, low resistance connectors ensure maximum output for the highest energy production.

* Please refer to Suntech Standard Module Installation Manual for details. **PV Cycle only for EU market.
*** Please refer to Suntech Product Near-coast Installation Manual for details. **** Please refer to Suntech Product Warranty for details.

www.suntech-power.com IEC-STD-Ve-NO1.01-Rev 2013

STP305 - 24/Ve
STP300 - 24/Ve
STP295 - 24/Ve
STP290 - 24/Ve

SUNTECH

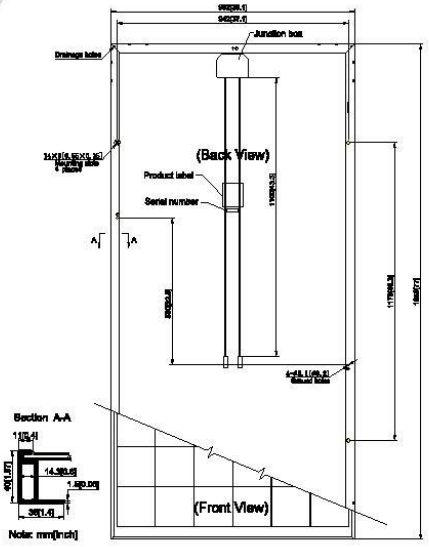

Electrical Characteristics

STC	STP305-24/Ve	STP300-24/Ve	STP295-24/Ve	STP290-24/Ve
Maximum Power at STC (Pmax)	305 W	300 W	295 W	290 W
Optimum Operating Voltage (Vmp)	36.2 V	35.9 V	35.6 V	35.4 V
Optimum Operating Current (Imp)	8.43 A	8.36 A	8.29 A	8.20 A
Open Circuit Voltage (Voc)	44.7 V	44.5 V	44.3 V	44.1 V
Short Circuit Current (Isc)	8.89 A	8.83 A	8.74 A	8.65 A
Module Efficiency	15.7%	15.5%	15.2%	14,9%
Operating Module Temperature	-40 °C to +85 °C			
Maximum System Voltage	1000 V DC (IEC)			
Maximum Series Fuse Rating	20 A			
Power Tolerance	0/+5 %			

STC: Irradiance 1000 W/m², module temperature 25 °C, AM=1.5;
Best in Class AAA solar simulator (IEC 60904-9) used, power measurement uncertainty is within +/- 3%

NOCT	STP305-24/Ve	STP300-24/Ve	STP295-24/Ve	STP290-24/Ve
Maximum Power at NOCT (Pmax)	222 W	219 W	216 W	212 W
Optimum Operating Voltage (Vmp)	32.6 V	32.4 V	32.2 V	32.1 V
Optimum Operating Current (Imp)	6.80 A	6.75 A	6.70 A	6.60 A
Open Circuit Voltage (Voc)	40.8 V	40.6 V	40.5 V	40.3 V
Short Circuit Current (Isc)	7.19 A	7.14 A	7.07 A	6.99 A

NOCT: Irradiance 800 W/m², ambient temperature 20 °C, AM=1.5, wind speed 1 m/s;
Best in Class AAA solar simulator (IEC 60904-9) used, power measurement uncertainty is within +/- 3%

Current-Voltage & Power-Voltage Curve (300-24)

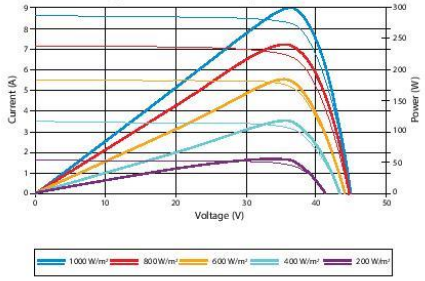

Excellent performance under weak light conditions: at an irradiation intensity of 200 W/m² (AM 1.5, 25 °C), 95.5% or higher of the STC efficiency (1000 W/m²) is achieved

Temperature Characteristics

Nominal Operating Cell Temperature (**NOCT**)	45±2°C
Temperature Coefficient of Pmax	-0.43 %/°C
Temperature Coefficient of Voc	-0.33 %/°C
Temperature Coefficient of Isc	0.067 %/°C

Mechanical Characteristics

Solar Cell	Polycrystalline silicon 156 × 156 mm (6 inches)
No. of Cells	72 (6 × 12)
Dimensions	1956 × 992 × 40mm (77.0 × 39.1 × 1.6 inches)
Weight	22 kgs (48.4 lbs.)
Front Glass	Tempered glass
Frame	Anodized aluminium alloy
Junction Box	IP67 rated (3 bypass diodes)
Output Cables	TUV (2Pfg1169:2007)
	4.0 mm² (0.006 inches²), symmetrical lengths (-) 1100mm (43.3 inches) and (+) 1100 mm (43.3 inches)
Connectors	H4 connectors

Dealer information

Packing Configuration

Container	40' HC
Pieces per pallet	25
Pallets per container	22
Pieces per container	550

Information on how to install and operate this product is available in the installation instruction. All values indicated in this data sheet are subject to change without prior announcement. The specifications may vary slightly. All specifications are in accordance with standard EN 50380. Color differences of the modules relative to the figures as well as discolorations of/in the modules which do not impair their proper functioning are possible and do not constitute a deviation from the specification.

E-mail: sales@suntech-power.com

[Annex 3] Code extraction from SODA for hourly granularity daily horizon

```
%%Parameters definition
Time = '04120000';
Time2 = '04110000';
Time3 = '04130000';
Year = '2017';
Dure = '5';


%%Saving of data
i = 10000;
while i <11500
   Name = num2str(i)
   D = str2double(Dure)

%Creation of the .BAT file
file = 'CarpentrasGranu.bat'; %Name of the .BAT file
fid = fopen(file,'wt'); %Open the .BAT file and allow editing

   %Text inside the .BAT file
   line1 = ['wget -O Forecast1' Dure '_CarpentrasGRANU0000000000000' Name '.csv  --header="soda-
user: guest" --header="soda-passwd: guest" "http://www.soda-
is.com/pub/hc3v4_similarity_forecast.php?geopoint=44.083,5.059&elevation=-999&firstday=' Year '-'
Time(1:2) '-' Time(3:4) '&lastday=' Year '-' Time3(1:2) '-' Time3(3:4) '&duration=' Dure
'&time=TU&slope=25&azimuth=180&albedo=0.2&horizon=1"'];
   line2 = ['wget -O Realtime1' Dure 'CarpentrasGRANU000000000000' Name '.csv  --header="soda-user:
guest" --header="soda-passwd: guest" "http://www.soda-
is.com/pub/hc3v4_forecast.php?geopoint=44.083,5.059&elevation=-999&firstday=' Year '-' Time2(1:2)
'-' Time2(3:4) '&lastday=' Year '-' Time(1:2) '-' Time(3:4) '&duration=' Dure
'&time=TU&slope=25&azimuth=180&albedo=0.2&horizon=1"'];

%Stick all text together
auto = {line1, line2};

%Print the text in the .BAT file
fprintf (fid, '%s\n', auto{:});

%End of the process
fclose (fid);

%Open the .BAT file to execute program and create .csv file
command = file;
status = system(command);

% end
pause(900); %Time waited between two consecutive extractions of .csv files
i = i + 25; %Go to the next extraction process
end
```

UNIVERSITAT POLITÈCNICA DE CATALUNYA BARCELONATECH

telecom BCN

[Annex 4] SODA similarity model

Solar Similarity Forecast: satellite-derived HelioClim-3 version 4 radiation values provided at « d+1 »

soda solar radiation data

*** http://www.soda-pro.com ***

Partners

TRANSVALOR

MINES ParisTech

ARMINES

Authors - speaker

Alexandre Boilley
TRANSVALOR

Claire Thomas
TRANSVALOR

Etienne Wey
TRANSVALOR

Mathilde Marchand
TRANSVALOR

Philippe Blanc
MINES ParisTech

Special offer

Free and unlimited access to this service
until the end of 2015

Contact us:
support-sales@soda-is.com

Photovoltaic plant owners are more and more urged **to predict what they will produce to ensure the load balancing of the electricity network**. A new solar forecast algorithm, named **Solar Forecast Similarity Method**, has been developed to predict irradiance for the next day based on a **statistical analysis of the long term HelioClim-3 version 4 (HC3v4) irradiation database**.

Method

- Compare today's Global Horizontal Irradiance (GHI) to the past 4 years (optimal learning period) HC3v4 irradiance database, and then:

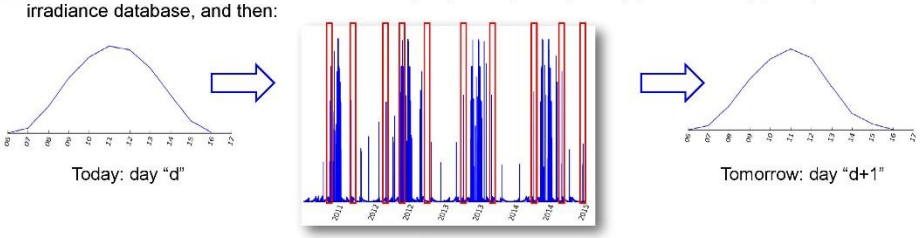

Today: day "d"

Tomorrow: day "d+1"

Detect the 10 similar days in the past based on square distance → Then, average the irradiation values of the days following the 10 selected days to produce the prediction

- More information on: *http://www.soda-pro.com/soda-products/hc3-similarity-forecast*
- Use the online interface: *http://www.soda-pro.com/web-services/radiation/helioclim-3-forecast*

Validation protocol and results

Validation protocol

- Comparison of the Similarity forecast GHI values against the measurements of Baseline Solar Radiation Network (BSRN) stations
- Compute: bias, Root Mean Square Error (RMSE), and correlation coefficient (CC) for each summarization: 15 min, 1h (see table below), 1 day, 1 month

BSRN data quality check

- Remove night and non plausible data
- Missing values: sum the available 15 min data to generate partial hourly, daily and monthly values
- 14 BSRN stations in the HC3v4 coverage, but only 9 stations with at least 4 years of data available

Ex. of 2-D histogram

BSRN station of Carpentras, 1 hour summarization

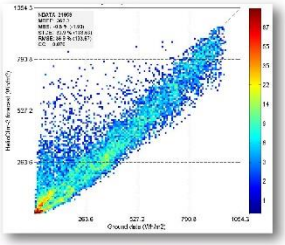

1 HOUR COMPARISON RESULTS Station	Number of values	Mean - BSRN - (Wh/m²)	Bias HC3v4 (Wh/m²) (relative in %)	Bias Forecast (Wh/m²) (relative in %)	RMSE HC3v4 (Wh/m²) (relative in %)	RMSE Forecast (Wh/m²) (relative in %)	Correl. coeff. HC3v4	Correl. coeff. Forecast
Toravere	18095	221.9	-6.0 (-2.7%)	-3.3 (-1.5%)	60.3 (27.2%)	126.5 (57.0%)	0.958	0.800
Cabauw	22886	249.6	-9.0 (-3.6%)	-10.8 (-4.3%)	56.7 (22.7%)	126.9 (50.8%)	0.968	0.821
Palaiseau	19680	285.1	9.3 (3.3%)	6.6 (2.3%)	51.4 (18.0%)	134.1 (47.1%)	0.978	0.830
Payerne	10167	306.7	-24.3 (-7.9%)	-31.6 (-10.3%)	67.3 (22.0%)	144.3 (47.1%)	0.970	0.839
Carpentras	21959	362.3	3.5 (1.0%)	-1.9 (-0.5%)	47.2 (13.0%)	133.7 (36.9%)	0.986	0.878
Sede Boqer	14417	505.6	-35.3 (-7.0%)	-39.0 (-7.7%)	69.2 (13.7%)	98.0 (19.4%)	0.982	0.957
Tamanrasset	20996	479.2	0.7 (0.1%)	0.4 (0.1%)	71.7 (15.0%)	120.6 (25.2%)	0.974	0.926
Brasilia	9428	417.1	16.4 (3.9%)	24.2 (5.8%)	110.4 (26.5%)	154.2 (37.0%)	0.933	0.860
Sao Martinho da Serra	11567	396.3	-5.8 (-1.5%)	-13.0 (-3.3%)	73.3 (18.5%)	190.6 (48.1%)	0.971	0.787

Conclusion and perspectives

SHC 2015 CONFERENCE DECEMBER 2-4 ISTANBUL, TURKEY

- The bias of the forecast is close to the HC3v4 bias
- RMSE can be up to 57% in cloudy areas, but correlation coefficients are almost always above 0.8
- This method performs better in slowly varying weather areas; in cloudy areas, numerical weather predictions at "d+1" will be used to constrain the choice of the nearest days in the HC3v4 database

SHC 2015, Istanbul, Turkey
2-4 Dec. 2015

Contact : support-sales@soda-is.com Site web : www.soda-pro.com

[Annex 5] Matlab code computation ETS

```
% Initialization
   % Constants to choose
L = 365;
j = 1;
alpha = 0.15;
beta = 0.005;
delta = 0.05;
filename = 'C:/Users/Cami/Desktop/20170511Test/Data20042016.xlsx';

% Initial Values
   % Initialization of the factors from
http://www.itl.nist.gov/div898/handbook/pmc/section4/pmc435.htm
Y = xlsread(filename, 'Data', 'C2:C4385');
obs = size(Y,1); % Length of the observations vector
I = zeros(L,1); % Stationnarity initial values
E = zeros(L,1); % Exponential smoothing final values
T = zeros(L,1); % Trend final values
S = zeros(L,1); % Stationnarity final values
F = zeros(L+j,1); % Forecasted final values

%fore = zeros(L,1);
Nseasons = floor(obs/L); % Number of seasons considered
seasonavg = zeros(Nseasons,1); % Empty vector to store the avg values for each season
averageobs = zeros(Nseasons,1); % Empty vector to store the avg of "each row"

      % Initialization the Exponential value
   E1 = Y(1,1);

      % Initialization of the Trend factor
   T0 = 0;
   for i = 1:L
      T0 = T0 + Y(L+i) - Y(i);
   end
   T1 = ((1/L)^2)*T0;

      % Initialization of the Seasonal factors
         % Computation of the average of each period

   for i = 1:Nseasons % We go through all the seasons
      for j = 1:L % For each period considered
         seasonavg(i,1) = seasonavg(i,1) + Y((i-1)*L+j); % We compute the sum of the values of Y for this
period
      end
      seasonavg(i,1) = seasonavg(i,1)/L; % We average each of these sums
   end

         % We devide the observation by their appropriate mean
   for  i = 1:Nseasons
      for j = 1:L
         averageobs((i-1)*L+j) = Y((i-1)*L+j)/seasonavg(i,1);
```

```
    end
  end

    % We compute the seasonal factors by computing the average of
    % each row
  for i = 1:L
    for j = 1:Nseasons
      I(i,1) = I(i,1)+averageobs((j-1)*L+i);
    end
    I(i,1) = I(i,1)/Nseasons;
  end


% Forecast Computation
  % Initialization
    E(1,1) = E1;
    T(1,1) = T1;

    for i = 1:L
      S(i,1) = I(i,1);
    end


for k = 2:obs

  % Exponential smoothing
if (k-1>=L)
  E(k,1) = alpha * (Y(k,1) - S(k-L,1)) + (1-alpha) * (E(k-1,1) + T(k-1,1));
else
  E(k,1) = alpha * (Y(k,1)) + (1-alpha) * (E(k-1,1) + T(k-1,1));
end
  % Trend smoothing
  T(k,1) = beta * (E(k,1) - E(k-1,1)) + (1-beta) * T(k-1,1);

  % Seasonal smoothing
  if (k-L>0)
  S(k,1) = delta * (Y(k,1) - E(k,1)) + (1-delta) * S(k-L,1);
  end

  % Forecast smoothing
    if (k+j-1>=L)
    F(k+j,1) = E(k,1)+j*T(k,1)+S(k-L+j);
    end
end
```